UPPSALA
UNIVERSITET

Digital Comprehensive Summaries of Uppsala Dissertations from the Faculty of Medicine 738

The Role of Mitochondrial Uncoupling in the Development of Diabetic Nephropathy

MALOU FRIEDERICH PERSSON

ACTA
UNIVERSITATIS
UPSALIENSIS
UPPSALA
2012

ISSN 1651-6206
ISBN 978-91-554-8266-4
urn:nbn:se:uu:diva-167815

Dissertation presented at Uppsala University to be publicly examined in B42, Biomedical Center, Uppsala. Friday, March 16, 2012 at 09:15 for the degree of Doctor of Philosophy (Faculty of Medicine). The examination will be conducted in English.

Abstract
Friederich Persson, M. 2012. The Role of Mitochondrial Uncoupling in the Development of Diabetic Nephropathy. Acta Universitatis Upsaliensis. *Digital Comprehensive Summaries of Uppsala Dissertations from the Faculty of Medicine* 738. 74 pp. Uppsala. ISBN 978-91-554-8266-4.

Diabetes is closely associated with increased oxidative stress, especially originating from the mitochondria. A mechanism to reduce increased mitochondria superoxide production is to reduce the mitochondria membrane potential by releasing protons across the mitochondria membrane. This phenomenon is referred to as mitochondria uncoupling since oxygen is consumed independently of ATP being produced and can be mediated by Uncoupling Proteins (UCPs). However, increased oxygen consumption is potentially detrimental for the kidney since it can cause tissue hypoxia. Therefore, this thesis aimed to investigate the role of mitochondria uncoupling for development of diabetic nephropathy.

UCP-2 was demonstrated to be the only isoform expressed in the kidney, and localized to tubular segments performing the majority of tubular electrolyte transport. Streptozotocin-induced diabetes in rats increased UCP-2 protein expression and correlated to increased non-transport dependent oxygen consumption in isolated proximal tubular cells. These effects were prevented by intense insulin treatment to the diabetic animals demonstrating a pivotal role of hyperglycemia. Importantly, elevated UCP-2 protein expression increased mitochondria uncoupling in mitochondria isolated from diabetic kidneys. Mitochondria uncoupling and altered morphology was also evident in kidneys from db/db-mice, a model of type-2 diabetes, together with proteinuria and glomerular hyperfiltration which are both clinical manifestations of diabetic nephropathy. Treatment with the antioxidant coenzyme Q10 prevented mitochondria uncoupling as well as morphological and functional alterations in these kidneys. Acute knockdown of UCP-2 paradoxically increased mitochondria uncoupling in a mechanism involving the adenosine nucleotide transporter. Increased uncoupling via adenosine nucleotide transporter decreased mitochondria membrane potential and kidney oxidative stress but did not affect glomerular filtration rate, renal blood flow, total kidney oxygen consumption or intrarenal tissue oxygen tension.

The role of increased mitochondria oxygen consumption was investigated by administering the chemical uncoupler dinitrophenol to healthy rats. Importantly, increased mitochondria oxygen consumption resulted in kidney tissue hypoxia, proteinuria and increased staining of the tubular injury marker vimentin, demonstrating a crucial role of increased oxygen consumption *per se* and the resulting kidney tissue hypoxia for the development of nephropathy.

Taken together, the data presented in this thesis establishes an important role of mitochondria uncoupling for the development of diabetic nephropathy.

Keywords: Kidney, mitochondria, Uncoupling Protein-2, Adenosine Nucleotide Transporter, uncoupling, diabetes, diabetic nephropathy, db/db, dinitrophenol, Coenzyme Q10, oxygen, rats, mice

Malou Friederich Persson, Uppsala University, Department of Medical Cell Biology, Integrative Physiology, Box 571, SE-751 23 Uppsala, Sweden.

ISSN 1651-6206
ISBN 978-91-554-8266-4
urn:nbn:se:uu:diva-167815 (http://urn.kb.se/resolve?urn=urn:nbn:se:uu:diva-167815)

Preface

"Into the wilderness". That was my thought when I started the journey toward my dissertation several years ago. Make no mistake, the thought still applies today but the day I don't feel lost is the day when I will quit the art of science! The journey has been hard but wonderful and I can proudly say that I am now better friends with the other wilderness inhabitants; the mad Computer, the small Rat, the enigmatic Mitochondria and the omnipresent Worry.

This work represents me and I hope you can glean something from it (perhaps just a laugh or two). Mark Twain said that a classic is a book that everybody wants to have but no one wants to read. As any good author would do, I will let you draw your own conclusions about the potential classical status of this work.

A true mitochondriac,

The white rabbit. Original illustration by John Tenniel from Alice's Adventures in Wonderland by Lewis Carroll, 1865.

Cover art

"The power of flight" by Odra Noel. Reprinted with permission. For more wonderful mitochondria and scientific art, please visit www.odranoel.eu.

List of papers

This thesis is based on the following papers, which are referred to in the text by their Roman numerals.

I **Identification and distribution of Uncoupling Protein isoforms in the normal and diabetic rat kidney.**
Friederich M*, Nordquist L*, Olerud J, Johansson M, Hansell P and Palm F. *Advances in Experimental Medicine and Biology* 2009, 645:205-212.

II **Diabetes-induced up-regulation of Uncoupling Protein-2 results in increased mitochondrial uncoupling in kidney proximal tubular cells.**
Friederich M, Fasching A, Hansell P, Nordquist L and Palm F. *Biochimica et Biophysica Acta* 2008, 1777(7-8):935-940.

III **Coenzyme Q10 prevents GDP-sensitive mitochondria uncoupling, glomerular hyperfiltration and proteinuria in kidneys from db/db-mice as a model of type 2 diabetes.**
Friederich Persson M, Franzén S, Catrina S-B, Dallner G, Hansell P, Brismar K and Palm F. *Diabetologia* 2012, in press.

IV **Acute knockdown of Uncoupling Protein-2 increases mitochondria uncoupling via the Adenine Nucleotide Transporter and decreases oxidative stress in diabetic kidneys.**
Friederich Persson M, Aslam S, Nordquist L, Welch WJ, Wilcox CS and Palm F. *Public Library of Science One* 2012, in revision.

V **Kidney function after *in vivo* gene silencing of Uncoupling Protein-2 in streptozotocin-induced diabetic rats.**
Friederich Persson M, Welch WJ, Wilcox CS and Palm F. *Advances in Experimental Medicine and Biology*, 2012, in press.

VI **Increased mitochondria uncoupling results in kidney tissue hypoxia and proteinuria.**
Friederich Persson M, Nangaku M, Fasching A, Hansell P and Palm F. 2012, *manuscript*.

Reprints were made with permission from the respective publishers.
* These authors contributed equally to the study.

Contents

Abbreviations

ADP	adenosine diphosphate
ANT	adenosine nucleotide transporter
ATP	adenosine triphosphate
BSA	bovine serum albumin
Ca^{2+}	calcium ion
CAT	carboxyatractylate
CKD	chronic kidney disease
CoQ10	coenzyme Q10
db/db	diabetes/diabetes
DNP	dinitrophenol
ESRD	end-stage renal disease
ETC	electron transport chain
$FADH_2$	reduced 1,5-dihydro-flavin adenine dinucleotide
FCCP	carbonylcyanide-p-trifluoromethoxyphenylhydrazone
FITC	fluorescein isothiocyanate
FMN	flavin mononucleotide
GDP	guanosine diphosphate
GFR	glomerular filtration rate
H_2O_2	hydrogen peroxide
HEPES	4-(2-hydroxyethyl)-1-piperazineethanesulfonic acid
HIF	hypoxia inducible factor
HRP	horseradish peroxidase
NADH	reduced nicotineamide adenine dinucleotide
$O_2^{\bullet -}$	superoxide radical
$OH^{\bullet -}$	hydroxyl radical
PAH	para-aminohippuric acid
PBS	phosphate buffered saline
ROS	reactive oxygen species
SDS	sodium dodecyl sulphate
siRNA	small interference ribonucleic acid
SOD	superoxide dismutase
TMRM	tetramethyl rhodamine methylester
TNa^+	tubular sodium transport
UCP	uncoupling protein

Introduction

The kidney

The mammalian kidney consists of approximately one million functional units, nephrons, performing filtration, reabsorption and secretion to produce the final urine. The kidney regulates body homeostasis in terms of electrolyte concentration, blood pressure, acid-base balance and excretion of waste products. The nephron is divided into the glomerulus, proximal tubule, loop of Henle, distal tubule and cortical and medullary collecting duct. The glomerulus filters electrolytes and nutrients but not cells and large proteins, forming the primary urine. The proximal tubule reabsorbs a majority of electrolytes and all glucose. The loop of Henle creates a hyperosmotic environment in the medulla, enabling the production of concentrated urine. The distal tubule and the collecting ducts are the main hormonal regulatory sites for electrolyte homeostasis and acid-base balance. Each nephron is surrounded by peritubular capillaries, oxygenating tubular cells and taking up reabsorbed electrolytes, nutrients and water.

Renal blood flow is high, equalling approximately 25% of cardiac output, resulting in a glomerular filtration rate (GFR) of approximately 125 ml/minute. This equals a primary urine production of 180 L/day; but after reabsorption along the nephron the final urine output is approximately 1.5 L/day, containing excess electrolytes and water-soluble waste products. Electrolytes, acids and bases are either reabsorbed or secreted in order to effectively maintain body homeostasis. Although the kidneys only comprises 0.5% of the total body mass it accounts for up to 10% of the total body oxygen consumption, the majority of which is attributed to the basolaterally located Na^+/K^+-adenosine triphosphate (ATP)ase. The Na^+/K^+-ATPase creates a sodium gradient over the tubular lumen, constituting the main driving force for apical transport of electrolytes and glucose. Reabsorption of sodium constitutes approximately 85% of the total kidney oxygen consumption [1] and the remaining 15% is due to basal metabolism [2]. Inhibition of electrolyte transport results in decreased oxygen usage and increased tissue oxygen tension in the kidney [3]. At the first glance it appears that the kidney is well-matched in terms of oxygen delivery and demand. However, despite high renal blood flow and well-oxygenated venous blood [4] the kidney cortical tissue oxygen tension is low and the renal medulla is on the brink of hypoxia [5, 6]. This is due to the presence of a morphological oxygen diffu-

sion shunt from the arteries to the veins as they are in close contact, and oxygen is therefore bypassing the renal parenchyma [7, 8].

The kidney may fail acutely following exposure to nephrotoxic substances or trauma but progressive nephropathy also occurs over time in diseases such as diabetes and hypertension. Progressive decrease in kidney function is referred to as chronic kidney disease (CKD) and often results in end-stage renal disease (ESRD). A GFR below 10 ml/minute/1.73 m^2 leads to life-threatening states of metabolic acidosis, hyperkalemia, uremia and sepsis requiring renal replacement therapy in form of dialysis and/or kidney transplantation. Globally, 1,783,000 patients were treated for ESRD in 2004 [9].

The mitochondrion

The production of ATP occurs in the mitochondria inner membrane, in the electron transport chain (ETC). The ETC consists of four complexes, an ATP-synthase and an adenosine nucleotide transporter (ANT). In the ETC, reduced nicotineamide adenine dinucleotide (NADH) and 1,5-dihydro-flavin adenine dinucleotide ($FADH_2$) donate electrons to complex I (NADH-dehydrogenase) and II (succinate-dehydrogenase), respectively. In order to accept and transfer electrons, prosthetic groups such as ferrous-sulphur (Fe-S) centers, flavin mononucleotide (FMN), coenzyme Q (CoQ) and cytochromes are required. Electrons from complex I and II are transferred via prosthetic groups to CoQ that is oxidized in the Q-cycle of complex III (cytochrome c reductase), resulting in reduced cytochrome c. Cytochrome c then transfers electrons to complex IV (cytochrome c oxidase) to be utilized in the reduction of molecular oxygen to water (Fig. 1).

In complex I, III and IV electron transfer is coupled to proton translocation across the inner membrane into the intermembrane space, creating a membrane potential. The ATP-synthase releases protons along the gradient and utilizes the energy to produce ATP from adenosine diphosphate (ADP) and inorganic phosphate. ADP is translocated in and ATP out of the mitochondria via the ANT to sustain cellular ATP levels. Electron transfer through the ETC, translocation of protons and production of ATP in the mitochondria are together known as oxidative phosphorylation (Fig. 2). This is a highly efficient process: 20 protons are translocated for every four electrons required to reduce molecular oxygen and approximately 30 ATP is produced from one glucose molecule as a result of oxidative phosphorylation. This should be compared to only four ATP being produced during anaerobic conditions when oxidative phosphorylation does not occur.

$$NADH + H^+ + FMN \rightarrow NAD^+ + FMNH_2 \qquad \text{(A)}$$

$$FMNH_2 + (Fe-S)_{ox} \rightarrow FMNH^{\bullet} + (Fe-S)_{red} + H^+ \qquad \text{(B)}$$

$$FMNH^{\bullet} + (Fe-S)_{ox} \rightarrow FMN + (Fe-S)_{red} + H^+ \qquad \text{(C)}$$

$$QH_2 + 2H^+_{matrix} + 2Fe^{3+}_{cytC} \rightarrow Q + 4H^+_{IMS} + 2Fe^{2+}_{cytC} \qquad \text{(D)}$$

$$O_2 + 8H^+_{matrix} + 4Fe^{2+}_{cytC} \rightarrow 2H_2O + 4H^+_{IMS} + 4Fe^{3+}_{cytC} \qquad \text{(E)}$$

Figure 1. Electrons are donated from NADH and $FADH_2$ to flavin mono nucleotide (FMN) (A) and through to Fe-S centers in a two-step reaction (B and C). In complex I and II reaction A-C through several Fe-S centers ultimately results in the reduction of Q to QH_2. Complex I transfer four protons (H^+) to the intermembrane space (IMS) per two electrons. QH_2 enters the Q-cycle in complex III, resulting in reduced cytochrome c (cyt C) and translocation of four H^+ to the IMS (D). Reduced cyt C is utilized at complex IV in the reduction of molecular oxygen to water and translocation of four H^+ to the IMS (E). Accumulation of H^+ in the IMS constitutes the mitochondria membrane potential.

Approximately 20% of the total mitochondria oxygen consumption is uncoupled from ATP-production due to a basal leakage of protons into the mitochondria matrix, causing oxygen to be consumed without production of ATP. The level of mitochondria basal leak varies between tissues, correlates with ANT-content [10, 11] and has been estimated to contribute to approximately 20-35% of the resting metabolic rate in rats [12, 13].

Mitochondria not only regulate oxidative phosphorylation, but also regulate apoptosis and calcium (Ca^{2+}) homeostasis. The key component in the regulation of apoptosis is cytochrome c, that when released initiates intracellular signalling cascades, ultimately resulting in controlled cell death; apoptosis [14]. Ca^{2+} is a cytoplasmic signalling molecule and as mitochondria contain specialised influx and efflux pathways they effectively control Ca^{2+} release [15] and are important in amplifying and modulating the cytoplasmic Ca^{2+} signalling [16].

By regulating, among others, oxidative phosphorylation, apoptosis and Ca^{2+} homeostasis, mitochondria are in many ways the key to normal cell function and survival.

Oxidative stress

Increased levels of reactive oxygen species (ROS) results in DNA-mutations, dysfunction of enzymes and oxidation of cellular membranes, consequences known as oxidative stress. The most common ROS is the superoxide radical ($O_2^{\bullet -}$), the product from an electron reacting with molecular oxygen. Other ROS include the hydroxyl radical ($OH^{\bullet}$), peroxynitrite ($ONOO^{\bullet -}$) and hydrogen peroxide (H_2O_2). $O_2^{\bullet -}$ and $OH^{\bullet}$ are highly reactive and reacts closely within their production site. However, H_2O_2 is stabile and can diffuse across cellular membranes. Important cellular antioxidant systems include superoxide dismutase (SOD) and catalase. SOD exists in three isoforms based on three locations; extracellular, intracellular or mitochondria SOD. By containing metallic ions centers (either Cu-Zn or Mn) $O_2^{\bullet -}$ is metabolized to H_2O_2 and molecular oxygen. H_2O_2 is thereafter converted to water by catalase.

Complex I and complex III of the ETC are permanent sources of oxidative stress due to the formation of semistable radicals during electron transfer ($FMN^{\bullet}$ in complex I and $QH^{\bullet}$ in complex III) from which an electron may slip to molecular oxygen, forming $O_2^{\bullet -}$. Approximately 0.1 to 0.2% of the total mitochondria oxygen consumption is due to $O_2^{\bullet -}$ production under normal conditions [17-19]. It was first believed that production of $O_2^{\bullet -}$ during normal conditions was a cellular mistake without any specific function. However, recent studies have implicated ROS as important cellular signaling molecule because overexpression of antioxidant defense systems in mice results in developmental malformations and death at 10 days of age [20]. Mitochondria $O_2^{\bullet -}$ production is also a key component of normal angiogenesis and regulation of the hypoxia-inducible factor (HIF)-system [21-23]. Thus, supplement of antioxidants to patients may not be beneficial under all conditions. A meta-analysis of 67 low bias risk-trials revealed that antioxidant supplementation was associated with increased mortality [24] and another study was prematurely terminated due increased relative risk of mortality in the group receiving β-carotene and vitamin A [25]. It is possible that treatment with antioxidants disrupts vital signaling of disease defense mechanisms. Large, randomized studies to evaluate the effects of antioxidants in primary and secondary prevention are needed and beneficial effects in one disease may not directly correlate to the same beneficial effects during all conditions.

Diabetes mellitus

Type 1 diabetes mellitus, known as insulin-dependent diabetes, debuts at an early age and is caused by death of pancreatic β-cells from an autoimmune reaction, resulting in hyperglycemia due to the lack of insulin. Type 1 diabe-

tes treatment mainly consists of insulin replacement to maintain glycemic control. Type 2 diabetes mellitus, known as insulin-independent diabetes is caused by a resistance to insulin in peripheral tissues. Patients with type 2 diabetes are therefore both hyperinsulinemic and hyperglycemic. Type 2 diabetes commonly debuts in elderly people, but is often co-occurring with obesity, dyslipidemia and hypertension; symptoms that when co-existing often are referred to as the metabolic syndrome. The prevalence of metabolic syndrome is rapidly increasing and approximately one third of middle-aged men and women have metabolic syndrome in the USA [26].

The prevalence of diabetes mellitus worldwide is projected to increase from 171 million in 2000 to 366 million in 2030 [27] and with increased prevalence of diabetes comes increased incidence of diabetic complications, such as nephropathy.

Diabetic nephropathy

Approximately 30% of diabetic patients develop diabetic complications [28] and 45% of all ESRD cases are caused by diabetic nephropathy [29, 30]. Diabetic nephropathy is associated with premature death due to cardiovascular events [29, 31]. Patients in the first stages of diabetic nephropathy display glomerular hyperfiltration, a known predictor of disease progression [32-34], and albumin excretion of less than 30 mg/day. Proteinuria is one of the best independent predictors of disease progression as patients with higher proteinuria more rapidly fall in GFR [35, 36]. Progression to early diabetic nephropathy is characterized by development of microalbuminuria (30-300 mg/day), loss of GFR and structural alterations such as reduced glomerular filtration area, thickening of glomerular basement membranes, accumulation of extracellular matrix and tubulointerstitial changes [37-42]. Further progression to overt nephropathy include macroalbuminuria (>300 mg/day), aggravated structural changes including fibrosis and a further decline of GFR with levels as low as 30 ml/minute/1.73 m^2. Further progression results in the need of renal replacement therapy as the patients finally enter irreversible ESRD.

The level of hyperglycemia correlates with progression to nephropathy and retinopathy [43] and reducing glycosylated hemoglobin levels to below 7% decreases progression to diabetic nephropathy even 6-8 years after the conclusion of the study [44]. Also, improved glycemic control reduces loss of kidney function in proteinuric type 1 diabetic patients [45]. As there is no treatment to fully reverse already established diabetic nephropathy the benefits of strict glycemic control are clear.

The mechanisms underlying the development of diabetic nephropathy are presently unclear and the view of diabetic nephropathy as mainly a glomerular disease has shifted to a focus on the proximal tubule [46]. Importantly, tubulointerstitial damage has emerged as one of the best predictors of disease

progression [32]. Although many studies have focused on structural alterations as causes for diabetic nephropathy it is well known that even the earliest clinical manifestation of diabetic nephropathy often represent an already well established morphological renal injury [42]. It is therefore crucial to study early, often subtle functional alterations when trying to elucidate mechanisms implicated in the development of diabetic nephropathy. Indeed, early alterations in kidney metabolism occurring already before altered morphology can be detected have recently been highlighted as an important mechanism for the development of diabetic nephropathy [47].

Oxidative stress in the diabetic kidney

Oxidative stress is closely associated with hyperglycemia and diabetes [48-51], especially in the kidneys [52-54] where increased oxidative stress has been demonstrated to decrease tissue oxygen tension in the diabetic kidney [53]. The degree of diabetic complications is associated with poor glycemic control [55] and it has been demonstrated that metabolic control in db/db-mice reduces oxidative stress and prevents the development of diabetic nephropathy [56]. Antioxidant systems are compromised in diabetic kidneys of both rats and mice [52, 57, 58] and treatment with antioxidants is highly beneficial to reduce kidney damage in these animal models [52-54, 59, 60]. Also, the total antioxidant capacity is reduced in diabetic patients [61, 62] but studies with antioxidant supplements have failed to reveal beneficial effects [63, 64]. This is most likely reflecting an inability of antioxidants to reverse already established kidney injuries whereas antioxidant supplement in animal studies have started prior to or at the onset of diabetes.

Important sources of $O_2^{\bullet-}$ in diabetic kidneys include activated NADPH oxidase [52, 65, 66] and mitochondria [49, 67]. Importantly, normalization of the $O_2^{\bullet-}$ levels at the mitochondria surface blocked three major pathways of hyperglycemic-induced injury [49].

The diabetic mitochondrion – a source of oxidative stress

The ETC is a source of $O_2^{\bullet-}$ under normal conditions [17]. Hyperglycemia causes increased mitochondria $O_2^{\bullet-}$ production [49] due to the increased mitochondria membrane potential [68, 69]. Increased membrane potential results in reduced forward motion of electrons in the ETC, which prolongs the half-life of semi-stable intermediates in complex I and III. This results in increased probability of electrons slipping directly to molecular oxygen, resulting in the increased $O_2^{\bullet-}$ production. Indeed, several studies have demonstrated that increased membrane potential correlates to increased mito-

chondria $O_2^{\bullet-}$ production [67-71]. A vicious circle has been proposed in mitochondria in which the reactive $O_2^{\bullet-}$ causes oxidative damage to its mitochondria production site which further increases $O_2^{\bullet-}$ production [72]. A proposed defense mechanism against excessive mitochondria production of $O_2^{\bullet-}$ is mitochondria uncoupling [73, 74], which directly lowers the mitochondria membrane potential.

Mitochondria uncoupling – a mechanism to decrease oxidative stress

Uncoupling proteins

Several studies have reported that reduced mitochondria membrane potential decreases $O_2^{\bullet-}$ production [19, 49, 69, 75, 76], a process that can be mediated by uncoupling proteins (UCP). UCPs belong to the mitochondria anion carrier family and are known to exist in five isoforms. UCP-1 was the first isoform discovered and specifically localized to brown adipose tissue [77, 78]. UCP-2, sharing 59% sequence homology with UCP-1, is expressed in vast amounts in spleen and lung tissue, reflecting a high content of macrophages in these tissues [79]. UCP-2 has been identified in kidneys of humans [80], rats and mice [81, 82]. UCP-3, sharing 57% sequence homology with UCP-1, is primarily localized to skeletal muscle and heart [83]. UCP-4 and -5 are mainly expressed in the brain [81, 84, 85] although low levels of mRNA can be detected in other tissues [81].

UCPs are inhibited by purine nucleotides, such as guanosine diphosphate (GDP) [86-88], but also by removal of fatty acids [89]. Two mechanisms are proposed to the function of UCPs: a proton channel [90] or cycling of fatty acids [91]. Both mechanisms describe the release of protons to the matrix independently of ATP production, which reduces the mitochondria membrane potential. The proposed fatty acid cycling mechanism stipulates that protonated fatty acids in the intermembrane space pass across the membrane, deprotonates in the mitochondria matrix and are translocated back into the intermembrane space by UCPs and the cycle starts all over again. Klingenberg *et al.* reported that the fatty acid palmitate modified with a hydrophilic glucose could not be translocated but the protonophoric action of UCP-1 was retained. This would support the proton channel hypothesis. However, this report was published in review papers [90, 92] and no original data or methods for fatty acid synthesis were ever published. The fatty acid cycling theory was first proposed Skulachev in 1991 [91] and has since then received considerable support [86, 93-95]. Importantly, Breen *et al.* performed a study demonstrating that palmitate modified with a hydrophilic glucose severely reduced the translocation of protons compared to unmodified palmitate and that GDP no longer had any effect. In that report, the fatty-acid cycl-

ing hypothesis was strongly supported as undecanesulfonate, a fatty acid unable to be protonated at neutral pH, could not sustain proton translocation but was in itself translocated by UCP-1 [96].

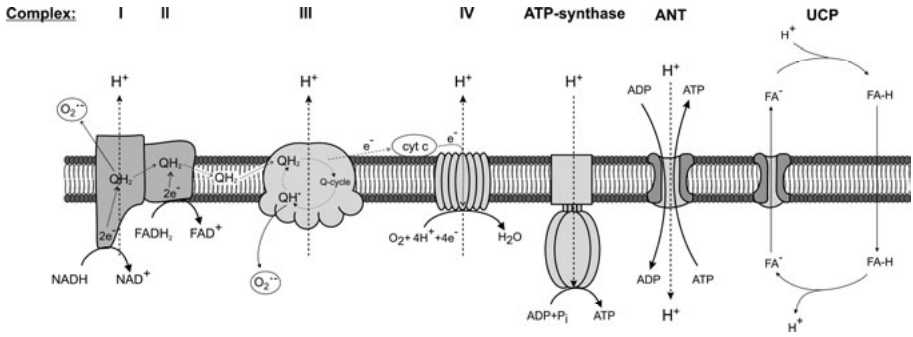

Figure 2. A summary of oxidative phosphorylation and $O_2^{\bullet-}$ production in the ETC under normal conditions. The proposed fatty acid cycling mechanism of uncoupling proteins is displayed to the right. ADP – adenosine diphosphate, ANT – adenosine nucleotide transporter, ATP – adenosine triphosphate, cyt c – cytochrome c, e^- – electron, FA^- – charged fatty acid, $FADH_2$ – reduced 1,5-dihydro-flavin adenine dinucleotide, FA-H – protonated fatty acid, H^+ – proton, NADH – reduced nicotineamide adenine dinucleotide, $O_2^{\bullet-}$ – superoxide radical, Pi – inorganic phosphate, QH_2 – reduced coenzyme Q, UCP – uncoupling protein. Modified from [74].

UCP-1 is important for non-shivering thermogenesis in response to cold [78] but studies have excluded a role for UCP-2 and -3 in thermogenesis since UCP-2 or -3 deficient mice display normal thermogenesis and response to cold [97, 98]. Instead, UCP-2 and -3 have been proposed to be protective against excessive mitochondria $O_2^{\bullet-}$ production. Yeast cells overexpressing UCP-2 have lower membrane potential [99] and oxidative stress levels correlate inversely with UCP-2 levels [76, 87]. In a study by Duval *et al*. antisense oligonucleotides against UCP-2 resulted in increased membrane potential and increased $O_2^{\bullet-}$ production in murine endothelial cells [76] and macrophages from UCP-2 knockout mice display elevated ROS production [97]. Immune cells display improved infection clearance rates and increased mitochondria $O_2^{\bullet-}$ production after siRNA to knockdown UCP-2 [100]. Also, UCP-2 knockout mice have higher survival rates following infections compared to corresponding control animals [97, 101]. Furthermore, UCP-2 prevents glucose-induced apoptosis in cultured neurons [102] and UCP-2 overexpression decreases brain lesion area and enhances neurological function after ischemic insults in mice [103].

Importantly, UCP-2 can be activated by $O_2^{\bullet-}$ and products of lipid peroxidation [104, 105], highlighting the potential of UCP-2 to be an effective regulator of $O_2^{\bullet-}$ production in mitochondria. UCP-2 protein levels are rapidly regulated due to a half-life of approximately 30 minutes [106], further strengthening the role of UCP-2 as a functional regulator of oxidative stress.

Uncoupling proteins and increased oxygen consumption

An important and potentially detrimental side effect of increased uncoupling via UCPs is increased mitochondrial oxygen consumption. Releasing protons independently of ATP-production via mitochondria uncoupling results in increased electron transfer down the ETC in order to sustain a sufficient ATP production. However, electrons transported along the ETC results in oxygen consumption and the amount of oxygen needed to sustain a sufficient ATP production will consequently increase [89]. This may reduce tissue oxygen tension and as oxidative stress both activates UCP-2 [89, 107] and causes reduced oxygen tension in the diabetic kidney [53] the role of UCP-2 in diabetic kidneys warrants further attention.

Oxygen handling in the diabetic kidney

The kidney tissue oxygen tension is low already under normal conditions [5, 6] and attempts to increase oxygen delivery via increased renal blood flow results in increased tubular load of electrolytes due to elevated GFR, which itself increases the metabolic demand. Consequently, any increase in kidney metabolism is likely to result in decreased kidney tissue oxygen tension. Indeed, increased kidney metabolism is associated with diabetic nephropathy [108] and diabetes is associated with a decreased kidney tissue oxygen tension in both animals and patients [54, 109-113]. Fine *et al.* proposed that an initial glomerular injury decreases blood flow through peritubular capillaries and result in decreased oxygenation of the kidney, promoting tubulointerstitial fibrosis and progression to kidney damage [114]. Indeed, loss of peritubular capillaries has been reported in diabetes [115]. Importantly, chronic tubulointerstitial hypoxia is acknowledged as a common pathway to ESRD [116-120].

Animal models of diabetes

Streptozotocin

Type 1 diabetes can be induced in mice and rats using streptozotocin ([2-deoxy-2(-3-methyl-nitrosourea-1-D-glucopyranose]) derived from *Streptomyces Achromogenes*. Streptozotocin consists of a nitrosamine group linked to a glucose molecule and was initially developed as a broad-spectrum antibiotic. However, it also induces β-cell death. It enters β-cells through insulin-independent glucose transporters and the nitrosamine decomposes to methyl ions which induce β-cells death and consequently insulin-dependent diabetes [121-123]. Streptozotocin is a well-known nephrotoxin but it has been demonstrated that streptozotocin *per se* does not cause alterations in kidney metabolism, function and growth in these animals when used appro-

priately [124]. Today, streptozotocin is widely used as a model for type 1 diabetes in both rats and mice. The animals exhibit transiently increased GFR [125], albuminuria [59] and structural alterations [126], symptoms that are shared with the clinical diabetic nephropathy.

Db/db-mice

A commonly used model of type 2 diabetes is the diabetes/diabetes (db/db)-mouse. Due to a deficient leptin signalling, these mice becomes hyperphagic with subsequent obesity, hyperglycemia and dyslipidemia after 8-10 weeks of age [56, 127, 128]. This model is insulin-independent and the mice develop hyperinsulinemia [129], albuminuria and increased GFR [130]. Diabetic nephropathy has been extensively studied in this model, focusing on structural alterations such as renal and glomerular hypertrophy [131], mesangial matrix expansion and albuminuria [132]. The db/db-mouse is presently suggested to be the best available model for diabetic nephropathy since it parallels the development of the human disease [133].

> "It's all very well to be able to write books but can you waggle your ears?" *JM Barrie (1860-1937)*

Aims

Increased mitochondria uncoupling in diabetic kidneys may be a double-edged sword; it may help to limit oxidative stress but may also reduce kidney tissue oxygen tension. The overall aim of this thesis was to investigate the role of mitochondria uncoupling for the development of diabetic nephropathy.

Specifically, the aims were:

Study I	To identify isoforms of UCP and investigate their distribution in control and diabetic rat kidneys.
Study II	To investigate the role of UCP-2 for mitochondria function and oxygen consumption in type 1 diabetic rat kidneys.
Study III	To investigate the role of mitochondria uncoupling in type 2 diabetic mouse kidneys and the role of oxidative stress in mediating the altered mitochondria and kidney function.
Study IV	To investigate the effect of acute knockdown of UCP-2 on mitochondria function in type 1 diabetic rat kidneys.
Study V	To investigate the effect of acute knockdown of UCP-2 on kidney function in type 1 diabetic rats.
Study VI	To investigate whether increased kidney oxygen consumption contributes to kidney damage independently of hyperglycemia and oxidative stress.

Materials and methods

Animals and chemicals (Study I-VI)

All chemicals were from Sigma-Aldrich (St Louis, MO, USA) of the highest grade available unless otherwise stated. Male Wistar-Furth rats (B&K, Sollentuna, Sweden, study I) and Sprague-Dawley rats were purchased from (Scanbur, Sollentuna, Sweden, study II, Charles River Laboratories, Wilmington, MA, USA, study IV and V, or Charles River, Sulzfeldt, Germany, study VI). BKS.Cg-Dock7m$^{+/+}$Leprdb/J (db/db)-mice and corresponding age-matched heterozygous littermates (control) were bred at the Karolinska Institute, Stockholm, Sweden (study III). Animals had free access to water and standard rat chow (Ewos, Södertälje, Sweden in study I, II and VI, Harlan Laboratories, USA in study IV and V), and standard mouse chow (R70, LABFOR, Lantmännen, Sweden, study III). All animals were housed in a temperature and light controlled environment and were monitored for overall health and symptoms of distress. In study VI bodyweight gain was also monitored.

Animals were divided into the following groups (n=6-14 in each group):

Study I	Control and diabetes.
Study II	Control, diabetes and diabetes with insulin.
Study III	Control and diabetes with and without chronic coenzyme Q10 (CoQ10) administration.
Study IV, V	Control and diabetes with and without either scrambled small interference ribonucleic acid (siRNA) or siRNA against UCP-2.
Study VI	Control with either vehicle or dinitrophenol (DNP).

Animal procedures

All animal procedures were performed in accordance with the National Institutes of Health guidelines for the use and care of laboratory animals and approved by the Uppsala animal ethics committee (study I, II, III and VI) and the animal care and use committee at Georgetown University Medical Center (study IV and V).

Induction of diabetes with streptozotocin (Study I, II, IV and V) and insulin treatment (Study II)

Type 1 diabetes was induced by an injection of streptozotocin dissolved in 0.2 ml saline in the tail vein (study I; 45 mg/kg bw, study II; 55 mg/kg bw, study IV and V; 65 mg/kg bw). Animals were considered diabetic if blood glucose increased to ≥15 mmol/l within 24 hours and remained elevated. Blood glucose concentrations were determined with test reagent strips (MediSense, Bedford, MA, USA, or FreeStyle, Abbott, Almeda, CA, USA) from blood samples obtained from the cut tip of the tail.

Insulin treatment in study II (8 IU/kg bw subcutaneous; three times per 24 hours) was started the same day as induction of diabetes and carried out throughout the course of diabetes. Duration of diabetes was two weeks (study I, II), seven days (study III and IV) or four to six weeks (study III).

Administration of siRNA (Study IV and V)

Under isoflurane anesthesia (2% in 40% oxygen) a polyethylene catheter was inserted into in the carotid artery and a non-functional scrambled siRNA or siRNA targeting UCP-2 (100 µg/rat; id nr 50931, Ambion, Austin, TX, USA) was administered in a total volume of 6 ml 37°C sterile saline during 6 seconds. The carotid artery was ligated and the wound closed. siRNA was administered on day five of diabetes and all measurements of mitochondria and kidney function carried out two days thereafter.

***In vivo* kidney function (Study V and VI)**

Animals were sedated with an intraperitoneal injection of sodium thiobutabarbital (Inactin, 120 mg/kg bw non-diabetic animals, 80 mg/kg bw diabetic animals) and placed on a heating pad servo-rectally controlled to maintain rectal temperature at 37°C. Tracheotomy was performed and polyethylene catheters were placed in either the carotid artery (study VI) or femoral artery (study V) to allow monitoring of blood pressure (Statham P23dB, Statham Laboratories, Los Angeles, CA, USA) and blood sampling. A catheter was placed in the femoral vein to allow for infusion of saline (5 ml/kg bw/h non-diabetic animals, 10 ml/kg bw/h diabetic animals). The left kidney was exposed by a subcostal flank incision and immobilized in a plastic cup. The left ureter and bladder were catheterized to allow for timed urine collection and urinary drainage, respectively. A flow probe to measure renal blood flow (Transonic Systems Inc., Ithaca, NY, USA) was placed around the left renal artery in study VI. After surgery, the animal was allowed to recover for 40 minutes followed by a 40 minute experimental period at the end of which a blood sample was drawn from the renal vein to allow for blood gas analysis. Kidney tissue oxygen tension was measured using Clark-type oxygen electrodes (Unisense, Aarhus, Denmark) calibrated with air-equilibrated buffer solution to 228 µmol/l oxygen and $Na_2S_2O_5$-saturated buffer to zero. GFR and renal blood flow were measured by clearance of ^{14}C-inulin and ^{3}H-

para-aminohippuric acid (PAH, 185 kBq bolus followed by 185 kBq/kg bw/h, American Radiolabelled Chemicals, St Louis, MO, USA).

GFR was calculated as inulin clearance=($[inulin]_{urine}$*urine flow)/$[inulin]_{plasma}$ and renal blood flow in study V with PAH-clearance adjusted for the hematocrit assuming an extraction of 70%. Total kidney oxygen consumption (µmol/minute) was estimated from the arteriovenous difference in oxygen content (O_2ct=([Hemoglobin]*oxygen saturation*1.34 + blood oxygen tension*0.003))*total renal blood flow. Tubular sodium transport (TNa^+, µmol/minute) was calculated as follows: $TNa^+=[Na^+]_{plasma}$*GFR-UNaV, where UNaV is the urinary Na^+ excretion. TNa^+ per consumed oxygen was calculated as TNa^+/oxygen consumption.

Treatment with dinitrophenol (Study VI) and CoQ10 (Study III)

Treatment with DNP (30 mg/kg/day, 1 ml dissolved in 1.5% methyl cellulose) or vehicle was performed by gavage for 30 days. Treatment with CoQ10 was carried out for two or seven weeks by administrating food containing Q10 (1g per kg standard mouse chow; R70, LABFOR, Lantmännen, Sweden) *ad libitum*.

Metabolic cages (Study III)

Feces and urine production and excretion of sodium, potassium and proteins were measured by placing animals in metabolic cages for 24 hours. Urinary content of sodium, potassium and protein were multiplied by urine volumes and expressed as excretions per 24 hours.

GFR in conscious mice (Study III)

Conscious GFR was measured by the single bolus injection method of fluorescein isothiocyanate (FITC)-inulin clearance [134]. 2% FITC-inulin was dissolved in phosphate buffered saline (PBS, Medicago AB, Uppsala, Sweden) and dialyzed in PBS at 4°C overnight in a 1000 Da cut-off dialysis membrane (Spectra/Por® 6 Membrane, Spectrum Laboratories Inc, Rancho Dominguez, CA, USA). FITC-inulin was filtrated through 0.45 µm syringe filters, 0.2 ml injected in the tail vein and blood samples taken at 1, 3, 7, 10, 15, 35, 55 and 75 minutes. Plasma samples were added to 4-(2-hydroxyethyl)-1-piperazineethanesulfonic acid (HEPES) buffer (500 mmol/l, pH 7.4) and assayed for fluorescence (496 nm excitation and 520 nm emission, Safire II, Tecan Austria GmbH, Grödig, Austria). The exact FITC-inulin dose was calculated from syringe pre to post weight and FITC-inulin clearance was calculated using non-compartmental pharmacokinetic data analysis [135].

Isolation of proximal tubular cells (Study II)

Animals were sedated with an intraperitoneal injection of sodium thiobutabarbital (Inactin, 120 mg/kg bw non-diabetic animals, 80 mg/kg bw diabetic animals), placed on a heating pad and tracheotomy was performed. A polyethylene catheter was placed in the right carotid artery, perfused with 20 ml of ice-cold PBS, and the right renal vein was cut open in order to facilitate complete perfusion of the kidneys. The kidneys were rapidly excised and placed in buffer containing (in mmol/l: 113.0 NaCl, 4.0 KCl, 27.2 $NaHCO_3$, 1.0 KH_2PO_4, 1.2 $MgCl_2$, 1.0 $CaCl_2$, 10.0 HEPES, 0.5 Ca^{2+}-lactate, 2.0 glutamine, 50 U/ml streptomycin (VWR International, Stockholm, Sweden), pH 7.4, 300 mOsm/kg H_2O). For non-diabetic rats, the buffer contained 5.8 mmol/l glucose and for diabetic animals the buffer contained 23.2 mmol/l glucose.

Kidney cortex was minced through a metallic mesh-strainer and immediately placed in a cold buffer solution (cf. above) containing 0.05% (wt/vol) collagenase. Thereafter, the minced tissue was incubated at 37°C, while the buffer was equilibrated with 95% oxygen/5% carbondioxide with manual stirring at regular intervals. The cell suspension was allowed to cool on ice and thereafter filtered through graded filters with pore sizes of 180, 75, 53 and 38 µm, respectively. After filtration, the cells were pelleted using a low centrifugal force (100 x g for 4 minutes) and resuspended in collagenase-free buffer. The washing procedure was repeated three times to ensure that no collagenase remained in the final cell suspension.

Isolation of kidney mitochondria (Study II, III and IV)

Rats (study II and IV) were euthanized by decapitation, mice (study III) by cervical dislocation and kidneys immediately excised and placed in ice-cold isolation buffer A (in mmol/l: 250 sucrose, 10 HEPES, pH 7.4, 300 mOsm/kg H_2O). In study III and IV buffer A also included 0.1% (wt/vol) bovine serum albumin (BSA; further purified fraction V). Kidney cortex was dissected on ice and homogenized in ice-cold buffer A with a prechilled Potter-Elvehjem homogenizer rotating at 600-800 rpm. The homogenate was centrifuged at 600-800 x g, 10 minutes, 4°C and the supernatant transferred into new tubes and centrifuged at 8000 x g (study III and IV) or 14,500 x g (study II) for 5 minutes at 4°C. Resulting pellets were resuspended with buffer A and the latter centrifugation repeated. The final pellets were resuspended with buffer B (in mmol/l: 70 sucrose, 220 mannitol, 5 $MgCl_2$, 5 KPO_4^-, 10 HEPES, pH 7.4, 300 mOsm/kg H_2O) with and without 0.3% (wt/vol) BSA. Isolated mitochondria was collected and analyzed for UCP-2 protein expression. In study III and IV, buffer B was supplemented with 50 µmol/l sodium palmitate.

Measurement of oxygen consumption in proximal tubular cells (Study II)

A custom made thermostatically controlled (37°C) gas-tight plexi-glass chamber with a total volume of 1.1 ml continuously stirred with an air-driven magnetic stirrer was used to measure oxygen consumption in isolated proximal tubular cells. A modified Unisense 500 oxygen sensing electrode (Unisense, Aarhus, Denmark), calibrated with air-equilibrated buffer solution to 228 µmol/l oxygen and $Na_2S_2O_5$-saturated buffer to zero, was used to record the rate of oxygen disappearance. All experiments were performed with and without pre-incubation of 1 mmol/l ouabain, an inhibitor of the Na^+/K^+-ATPase. Oxygen consumption was calculated as the oxygen disappearance rate adjusted for protein concentration.

Measurement of oxygen consumption in isolated mitochondria

Hansatech system (Study II and IV)

Temperature-controlled chambers with continuous stirring and Clark-type electrodes (Hansatech Instruments, Kings Lynn, UK) calibrated with air-equilibrated buffer solution and $Na_2S_2O_5$-saturated buffer to zero was utilized. Mitochondria (0.5 mg/ml) were added in buffer B (c.f. above) with or without BSA and oxygen consumption recorded as the rate of oxygen disappearance corrected for cytochrome aa_3 content (study II) or protein concentration (study IV).

Oroboros system (Study III)

Oxygraph (O_2K, Oroboros Instruments, Innsbruck, Austria) calibrated with air-equilibrated buffer B and $Na_2S_2O_5$-saturated water with continuous stirring was used to measure oxygen consumption. Mitochondria were added in a final concentration of 0.2 mg/ml in 2.5 ml air-equilibrated buffer and oxygen consumption was recorded via DatLab software for Data Acquisition and Analysis (Oroboros Instruments, Innsbruck, Austria), calculating and displaying oxygen consumption as a function of oxygen disappearance. All measurements were adjusted for protein concentration.

Experimental protocols and calculations

ADP-stimulated oxygen consumption was estimated by addition of ADP (300 µmol/l, potassium salt, pH 7.4, containing 0.6 mol $MgCl_2$/mol ADP) to mitochondria energized with glutamate (10 mmol/l, sodium salt, pH 7.4).

Respiratory control ratio was calculated as oxygen consumption after ADP divided by the oxygen consumption after glutamate.

Mitochondria uncoupling was studied in the absence of ATP-synthesis as glutamate-stimulated oxygen consumption. Addition of glutamate (*i.e.* electron-donating NADH) increases the inner mitochondria membrane potential due to a transport of protons to the intermembrane space and any mechanism resulting in proton leak across the mitochondrial inner membrane (*i.e.* uncoupling) will be observed as increased oxygen consumption. Subsequent addition of the ATP-synthase inhibitor oligomycin mimics the effects of ADP-depletion and therefore provides a second indication of mitochondria uncoupling. Finally, the UCP inhibitor GDP was added to confirm the involvement of UCP for any observed mitochondria uncoupling.

In study III mitochondria were separately incubated for 30 minutes on ice with 12 µg oligomycin/mg protein, 0.5 mmol/l GDP, 50 µmol/l palmitic acid or a combination of oligomycin and GDP or palmitic acid and oxygen consumption analyzed. After each measurement, a sample from the chamber was frozen for later analysis of protein concentration. In study III sequential additions of mitochondria, glutamate, oligomycin and GDP were made and the oxygen consumption analyzed after each addition. Estimation of respiratory control ratio was performed in separate experiments.

Measurement of mitochondria ATP-production (Study IV)

Mitochondria ATP production was analyzed with a commercially available bioluminescence assay from Molecular Probes (ATP determination kit, Molecular Probes, Invitrogen, Paisley, UK) according to manufacturer's instruction. Analysis was performed in four settings: 1) mitochondria, glutamate and ADP, 2) mitochondria, glutamate, ADP and carbonylcyanide-p-trifluoromethoxyphenyl-hydrazone (FCCP), 3) mitochondria, glutamate, ADP and oligomycin, and 4) mitochondria, glutamate, ADP, oligomycin and carboxyatractylate (CAT). Samples were incubated for 3 minutes at 37°C and thereafter snap frozen in liquid nitrogen. ATP production was corrected for protein concentration and expressed as µmol ATP/minute/mg protein.

Measurement of mitochondria membrane potential (Study IV)

Mitochondria membrane potential was measured as uptake of the fluorofor tetramethylrhodamine methylester (TMRM) [136]. TMRM (0.35 µmol/l) was mixed with buffer B (c.f. above) and fluorescence measured at excitation 546 nm and emission 590 nm in a 384-well plate (GreinerBio One,

Frickenhausen, Germany), and denoted total TMRM ($TMRM_T$). Mitochondria incubated with oligomycin and glutamate or with coincubation of oligomycin, glutamate and GDP were added to the wells, incubated for 5 minutes and pelleted at 8000 x g for 10 minutes. The supernatant of each pellet was analyzed for fluorescence (TMRM outside; $TMRM_O$). Mitochondria uptake of TMRM was calculated as $TMRM_T$-$TMRM_O$ and corrected for protein concentration.

Determination of electrolytes, protein concentration and cytochrome aa_3 (Study II, III, IV, V and VI)

Urinary sodium and potassium excretions were determined by flame photometry (IL943, Instrumentation Laboratory, Milan, Italy) and urinary protein excretion by DC Protein Assay (Bio-Rad Laboratories, CA, USA). Cytochrome aa_3 content was determined as previously described [137]. In brief, 100 µl aliquots of the sample was added to 2% Triton-X-100 (Merck laboratories, Darmstadt, Germany) in 0.1 mol/l PBS (pH 7.4) with and without saturated amounts of $Na_2S_2O_5$. The oxidized-reduced absorbance spectrum was obtained at 605-630 nm, and the concentration determined using a millimolar extinction coefficient of 12 with adjustment for the dilution factor.

Polymerase chain reaction (Study I and VI)

Study I

Total RNA was isolated with the guanidinium-based lysis buffer method with RNAquous-4 PCR Kit (Ambion, Austin, TX, USA) and treated with DNaseI. Reverse transcriptase reactions were performed using Superscript III first strand cDNA synthesis (Invitrogen, Carlsbad, CA, USA). Amplification was obtained with a Lightcycler system (Roche-Diagnostic, Lewers, UK) using DyNAmo™ Capillary SYBR® Green qPCR Kit (Finnzymes, Espoo, Finland). β-actin was used as housekeeping gene and PCR products run through a 1.8% agarose gel for size identification.

Study VI

Total RNA was extracted from kidney homogenates with Isogen RNA isolation kit (Nippon Gene, Tokyo, Japan). Supercript II reverse transcriptase (Life Technologies BRL, Rockville, MD, USA) was used to synthesize cDNA from total RNA and levels were assessed by real-time quantitative PCR using SYBR green PCR reagent (Qiagen, Hilden, Germany) and the iCycler PCR system (Bio-Rad Laboratories, Hercules, CA, USA). β-actin

was used as a house keeping gene. Primer sequences for study I and VI are listed in Table 1.

Table 1. Primer sequences used in study I and VI. EPO – erythropoietin, GLUT-1 – glucose transporter 1, HIF-1α – hypoxia inducible factor-1α, HO-1 – heme oxygenase 1, UCP – uncoupling protein, VEGF – vascular endothelial growth factor.

Gene	Forward sequence	Reverse sequence	Product (bp)	Study
UCP-1	GTGAAGGTCAGAATGCAAGC	AGGGCCCCCTTCATGAGGTC	199	I
UCP-2	GCATTGGCCTCTACGACTCT	CTGGAAGCGGACCTTTACC	151	I
UCP-3	TGCAGCCTGTTTTGCTGATCT	GGGTTCTCCCCTTGGATCTG	80	I
β-actin	CCACCGATCCACACAGACTACTTG	GCTCTGCGTCCTAGCACC	76	I
EPO	TACGTAGCCTCACTTCACTGCTT	GCAGAAAGTATCCGCTGTGAGTGTTC	113	VI
GLUT-1	CAGTTCGGCTATAACACCGGTGTC	ATAGCGGTGGTTCCATGTTT	84	VI
HIF-1α	GTTTACTAAAGGACAAGTCACC	TTCTGTTTGTTGAAGGGAG	193	VI
HO-1	TCTATCGTGCTCGCATGAAC	CAGCTCCTCAAACAGCTCAA	110	VI
VEGF	TTACTGCTGTACCTCCAC	ACAGGACGGCTTGAAGATA	189	VI
β-actin	CTTTCTACAATGAGCTGCGTG	TCATGAGGTAGTCTGTCAGG	306	VI

Measurement of thiobarbituric reactive substances and malondialdehyde (Study IV)

Kidney cortex content of thiobarbituric reactive substances (TBARS) was measured by adding a 50 µl sample of kidney cortex homogenate to 500 µl hydrochloric acid (50 mmol/l), vortexing and adding 167 µl thiobarbituric acid (0.67%). After incubation (30 minutes, 95°C) the samples were cooled to room temperature and 667 µl methanol:n-butanol added (3:17 mix, prepared fresh). The sample was vortexed and centrifuged at 2500 rpm for 20 minutes at 18°C. The top layer was transferred to a transparent 384 well plate, analyzed for absorbance at 535 nm and corrected for protein concentration.

Free plasma malondialdehyde (MDA) was measured by high-performance capillary electrophoresis-Micellar Electrokinetic Chromatography. The plasma was filtered through a centrifugal filter with 3000 Da cut-off and the ultrafiltrate directly injected into an uncoated fused silica capillary (75 micron ID, length to detector 40 cm, total length 50.2 cm) on a Beckman Coulter MDQ system (Fullerton, CA, USA) equipped with a UV detector. A large stacking volume was used to introduce a large plug of the sample hydrodynamically (0.5 psi, 20 seconds). The background electrolyte solution contained (in mmol/l: 25 sodium tetraborate spermine, 1 HCl, 2 tetradecyltrimethylammonium bromide, pH 9.7). UV was detected 260 nm with methyl MDA as an internal standard. The separation was carried out at -12kV and 25°C. Intra-assay and inter-assay CV for this assay in samples of

plasma are 2.1% and 4.3% respectively and the limit of detection is 0.1 µmol/l.

Immunohistochemistry (Study I and VI)

Study I

Kidneys were fixed with 4% formaldehyde, dehydrated and embedded in paraffin. Sections (5 µm) were deparaffinized and immersed in ethanol with concentration gradients and thereafter heated in citrate solution (0.01 mol/l, pH 6.0) for antigen retrieval. Endogenous peroxidase activity was blocked using 3% H_2O_2 and non-specific binding was prevented by blocking with normal goat serum (Santa Cruz Biotechnology, Heidelberg, Germany). Thereafter, the sections were incubated with an antibody against UCP-2 in a 1:50 dilution overnight at 4°C. The sections were rinsed with tris-buffered saline tween-20 and incubated with a biotinylated secondary antibody against goat IgG (Santa Cruz Biotechnology; Heidelberg, Germany, 1:500). After rinsing, sections were incubated with an avidin biotin enzyme reagent (ABC Elite Kit; Vector laboratories, Burlingame, CA, USA) and labeling visualized using a peroxide substrate solution with 0.8 mmol/l 3,3-diaminobenzidine and 0.01% H_2O_2. The sections were subsequently counterstained with hematoxylin and mounted.

Study VI

Animals were anesthetized with Inactin and a polyethylene catheter placed in the carotid artery followed by infusion of 20 ml ice-cold PBS and the renal vein cut opened in order to facilitate complete drainage of the kidneys. The kidneys were dissected on ice and placed in methyl Carnoy's fixative (methanol:chloroform:acetic acid, 6:3:1) or snap frozen using liquid nitrogen. Carnoy-fixed tissue sections were paraffin-embedded and indirect immunoperoxidase methods were used to identify vimentin (a marker of tubular injury) using mouse monoclonal antibody V9 (Dako, Carpinteria, CA, USA) as described previously [138] and monocytes and macrophages using mouse monoclonal antibody ED-1 (Chemicon, Temecula, CA, USA) on 3 µm thick sections. Computer-based counting of ED-1 positive infiltrating cells was performed utilizing Image J software (NIH, Bethesda, MD, USA) and the number of vimentin positive tubules surrounded by healthy tubules was counted. Quantification was performed in a blinded manner using 20 randomly selected fields of cortex per cross-section (x100).

Western blotting (Study II, III, IV and V)

Samples were homogenized in 700 µl buffer (in mmol/l: 10 NaF, 80 Tris, 1.0% NP40, 0.5% sodium deoxycholate, 0.1% sodium dodecyl sulphate (SDS), pH 7.5) containing enzyme inhibitors (phosphatase inhibitor cocktail-2; 10 µl/ml, and Complete Mini; 1 tablet/1.5 ml; Roche Diagnostics, Mannheim, Germany). Equal amounts of protein was run on 12.5% Tris-HCl gels with Tris/glycine/SDS buffer and the proteins detected, after transfer to nitrocellulose membranes, using goat anti-rat UCP-2 antibody (1:1000; Santa Cruz Biotechnology, Santa Cruz, CA) and horse radish peroxidase (HRP)-conjugated secondary antibody (rabbit anti-goat, 1:10,000; Kirkegaard and Perry Laboratories, Gaithersburg, MD) by an ECL-camera (Kodak image station 2000; New Haven, CT). β-actin was detected using mouse anti-rat β-actin antibody (1:10,000) and secondary HRP-conjugated goat-anti mouse antibody (1:60,000; Kirkegaard and Perry Laboratories, Gaithersburg, MD). Protein levels analyzed in tissue homogenates were all corrected for β-actin. Western blot analysis of samples from isolated mitochondria was normalized to protein concentration.

Electron microscopy (Study III)

Thin slices of renal cortex from two animals of each group was fixed in 2.5% glutaraldehyde with sodium cacodylate buffer (150 mmol/l, pH 7.4), post fixed in 1% OsO_4 and embedded in Agar 100 Resin (Agar Scientific, Stansted, UK). Sections were contrasted with 2% uranyl acetate and Reynolds lead citrate solution and examined in a Hitachi 7100 transmission electron microscope (Tokyo, Japan). Electron micrographs were taken with a Gatan multiscan camera model 791 using Gatan digital software version 3.6.4 (Gatan, Pleasanton, USA). Representative mitochondria were selected by superimposing an 8x5 grid onto the micrographs and selecting those which were located in any intersection of the grids. Mitochondria size was determined by measuring the longest distance of each mitochondrion. Fragmentation was scored from 0 to 4 (0 representing no fragmentation to 4 representing full fragmentation). Percent intracellular content of mitochondria was also calculated. All mitochondria micrograph analyses were performed by the same blinded investigator.

Statistical considerations (Study I-VI)

In study I and VI, Student's t-test was used to compare means of two groups. In paper II, statistical comparisons were performed using one-way analysis of variance (ANOVA) followed by Fisher's PLSD test and multiple comparisons within the same group were performed using repeated measures

ANOVA followed by Dunnett's test for paired comparisons (Statview, Abacus Concepts, Berkeley, CA, USA). In study III, comparisons between groups were made using two-way analysis of variance (2by2-ANOVA). Statistical comparisons in study IV and V were made using ANOVA followed by Bonferroni's multiple comparisons test. Paired Student's t-tests were applied for comparisons within each group.

$P<0.05$ was considered statistically significant and analyses were performed using Graph Pad Prism software (Graph Pad Inc., San Diego, CA, USA) unless otherwise stated. All values are presented as mean±SEM.

Results

Identification and localization of Uncoupling Proteins in the kidney (Study I)

UCP-2 was identified as the only isoform expressed in rat kidneys using semi-quantitative PCR. Neither UCP-1 nor UCP-3 could be detected (Fig 3 and 4). By immunohistochemistry UCP-2 was localized to cells of the proximal tubule and of the medullary thick ascending limb of the loop of Henle. There was no staining in distal tubules, glomeruli or vascular bundles (Fig. 5).

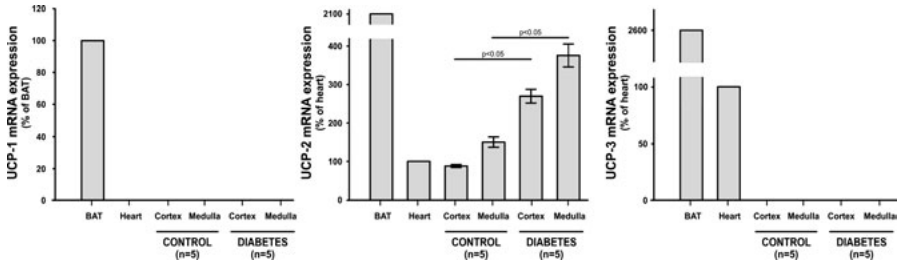

Figure 3. UCP-1 (left), UCP-2 (middle) and UCP-3 (right) mRNA expression in brown adipose tissue (BAT) and heart of normoglycemic rats and kidney cortex and medulla in normoglycemic and diabetic rats. All values are presented as mean±SEM.

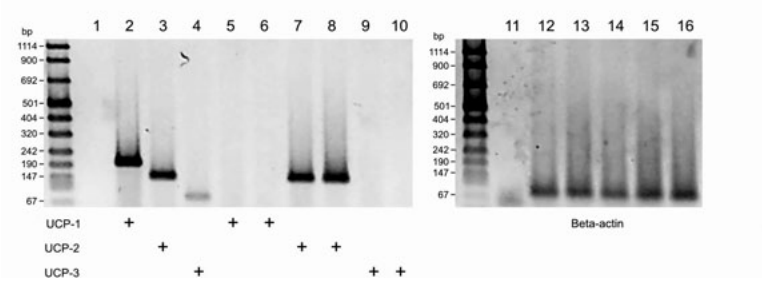

Figure 4. Left panel: PCR products from negative control (1), positive controls (2: UCP-1 in brown adipose tissue, 3: UCP-2 in kidney, 4: UCP-3 in heart) and kidney tissue (5, 7, 9: normoglycemic control and 6, 8, 10: diabetic) from rats. Right panel: β-actin content of negative control (11), brown adipose tissue (12), heart (13) and kidney samples (14-16).

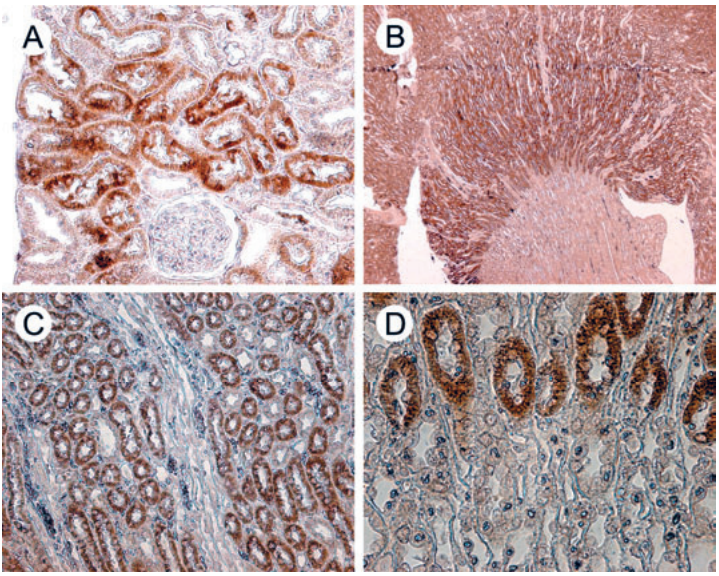

Figure 5. Immunohistochemical staining for UCP-2 in kidneys of normoglycemic rats. A) Staining of proximal tubular cells, but not glomerulus or cells in the distal nephron. B) Staining of outer medullary region. C) Staining of cells of the mTAL, but not vascular bundles. D) High magnification of mTAL cells positive for UCP-2, whereas no staining occurs in other cells of the loop of Henle.

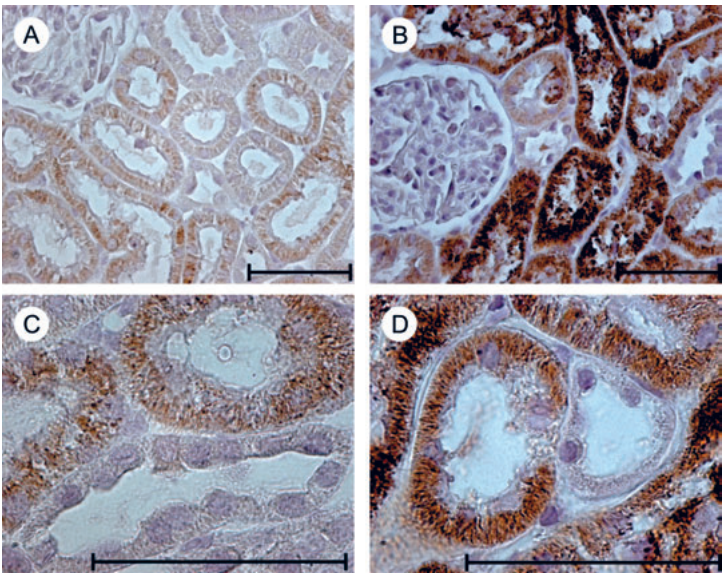

Figure 6. Immunohistochemical staining of UCP-2 in normoglycemic (A+C) and hyperglycemic rats (B+D). Horizontal black bars indicate 50 µm.

Oxygen consumption in isolated proximal tubular cells (Study II)

Kidney proximal tubular cells isolated from diabetic animals displayed increased total and transport-independent oxygen consumption compared to normoglycemic controls. Insulin treatment prevented all observed effects (Fig 7).

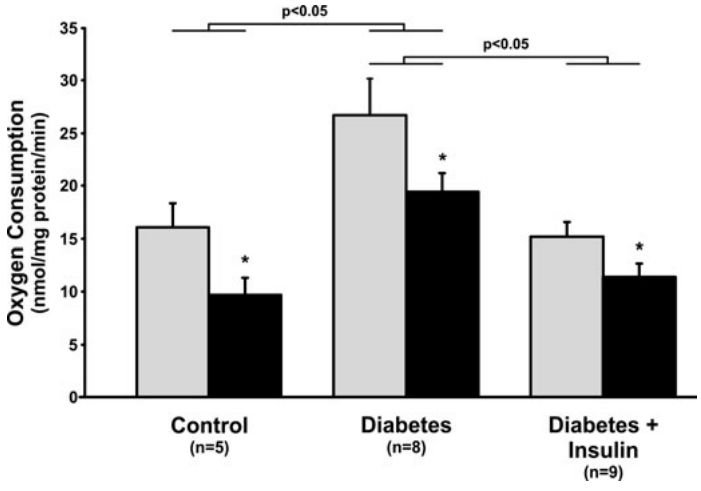

Figure 7. Oxygen consumption in proximal tubular cells from normoglycemic control and diabetic rats with and without intensive insulin treatment during baseline (grey bars) and ouabain treatment (black bars). All values are presented as mean±SEM. * denotes p<0.05 compared to untreated cells.

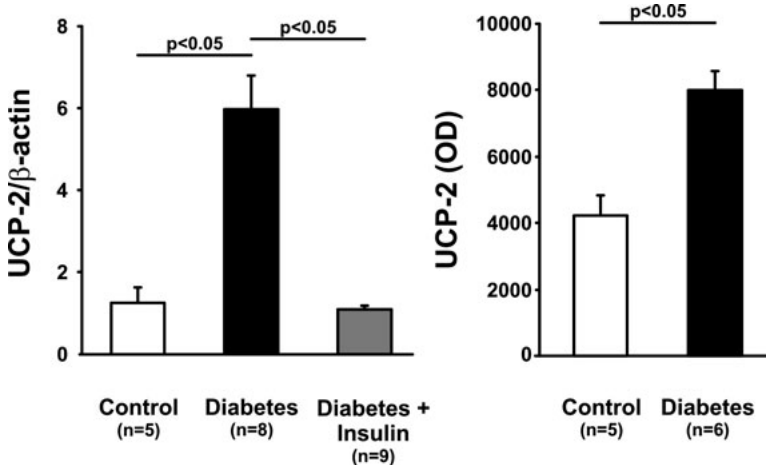

Figure 8. UCP-2 protein levels in kidney cortex homogenate (left) and isolated kidney cortex mitochondria (right). All values are presented as mean±SEM.

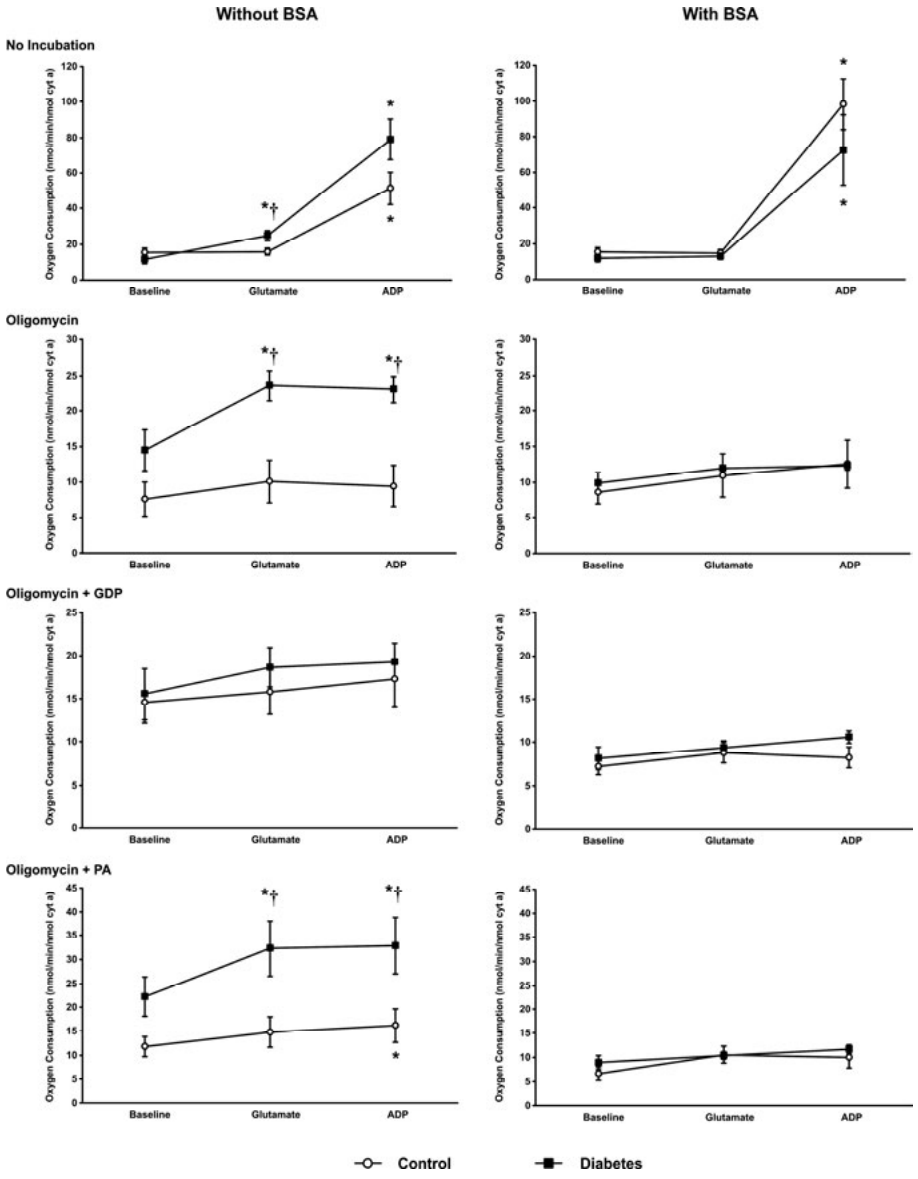

Figure 9. Oxygen consumption in mitochondria isolated from control and diabetic rat kidneys with and without bovine serum albumin (BSA) during baseline and after sequential addition of glutamate and ADP. The ATP-synthase was inhibited by oligomycin, UCPs were inhibited by guanosine diphosphate (GDP) and stimulated by palmitic acid (PA). All values are presented as mean±SEM. * denotes $P<0.05$ when compared to baseline within the same group and † denotes $P<0.05$ when compared to corresponding treatment within the control group.

Type-1 diabetes and mitochondria function (Study II)

Streptozotocin-induced diabetes increased UCP-2 mRNA levels, protein levels and immunohistochemical staining in proximal tubular cells and mTAL (Fig 3, 8 and 6). Increased protein levels of UCP-2 in kidney cortex of diabetic animals were prevented by insulin treatment and elevated UCP-2 protein expression was also confirmed in mitochondria isolated from diabetic rats (Fig 8).

Untreated mitochondria isolated from diabetic kidneys displayed increased glutamate-stimulated uncoupling compared to controls. This difference was retained after incubation with oligomycin but disappeared when GDP was present. Incubation with palmitic acid stimulated oxygen consumption in the presence of oligomycin but only in mitochondria from diabetic animals (Fig. 9; left panel). All differences between control and diabetic mitochondria were abolished when BSA was present in the media (Fig. 9; right panel).

Type-2 diabetes and mitochondria function (Study III)

Kidney mitochondria isolated from type 2 diabetic db/db-mice displayed increased glutamate-stimulated oxygen consumption that was inhibited by GDP. No effect of either glutamate or GDP was observed after CoQ10-treatment of db/db-mice or in control animals (Fig. 10). All animals had similar respiratory control ratios (Fig. 11). Also, db/db-mice displayed proteinuria and glomerular hyperfiltration, both of which were prevented by chronic treatment with CoQ10. Also, CoQ10 reduced proteinuria in control mice (Fig. 12).

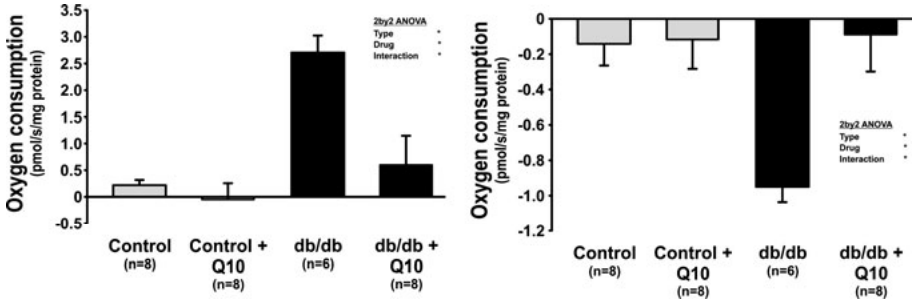

Figure 10. Glutamate-stimulated oxygen consumption (left) and GDP-inhibited oxygen consumption (right) in control and db/db-mice with and without treatment with CoQ10. All values are presented as mean±SEM. * denotes $P<0.05$

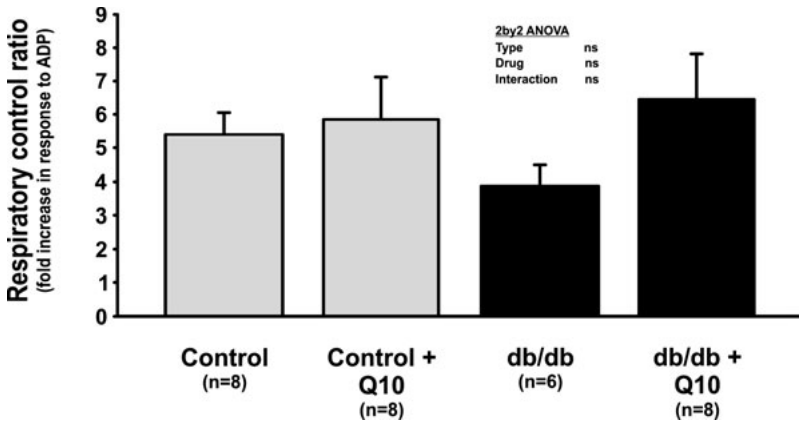

Figure 11. Respiratory control ratio of mitochondria from control and db/db-mice with and without treatment with CoQ10. All values are presented as mean±SEM.

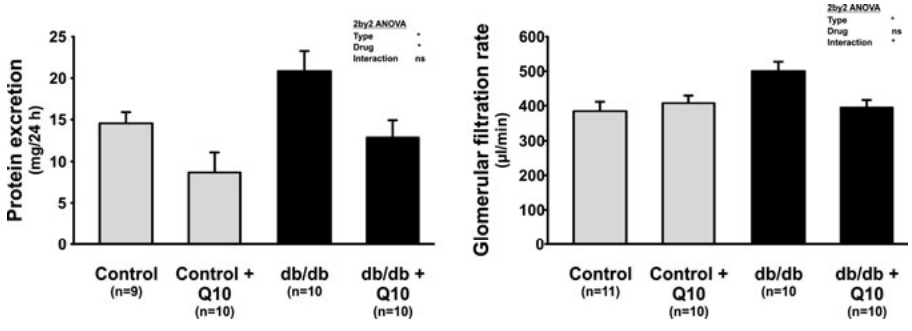

Figure 12. Protein excretion (left) and glomerular filtration rate (right) in control and db/db-mice with and without treatment with CoQ10. All values are presented as mean±SEM. * denotes $P<0.05$

Diabetes did not result in elevated UCP-2 protein levels in kidneys from db/db-mice. However, reduction of UCP-2 protein levels was observed after CoQ10-treatment in both control and db/db-mice. Untreated db/db-mice had elevated levels of protein carbonyls in kidney cortex, which was reduced by CoQ10-treatment (Fig. 13). Electron microscopy revealed increased cellular mitochondria content, size and fragmentation in db/db-mice, but CoQ10 only prevented the increased size and fragmentation (Table 2). Representative micrographs are shown in Fig. 14.

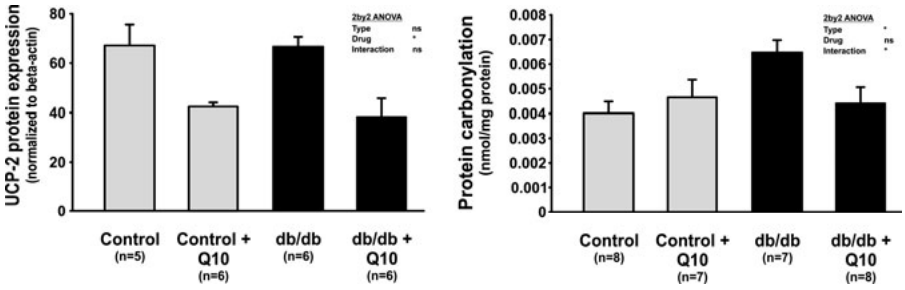

Figure 13. UCP-2 protein levels (left) and level of protein carbonlyation (right) in kidney cortex homogenate in control and db/db-mice with and without treatment with CoQ10. All values are presented as mean±SEM. * denotes P<0.05.

Table 2. Mitochondria size, fragmentation score and cellular content of mitochondria in control and db/db-mice with and without treatment with CoQ10. * denotes P<0.05.

	Mitochondria size (µM)	N of analysed images	N of analysed mitochondria	Fragmentation score (1-4)	N of analysed images	Cell mitochondria content (%)	N of analysed images
Control	1±0.0	49	1003	0.7±0.1	53	41.0±3.4	10
Control + Q10	1.2±0.0	31	619	0.9±0.2	31	37.2±4.1	7
db/db	1.6±0.1	26	509	2.4±0.3	26	47.6±2.5	9
db/db + Q10	0.96±0.0	32	521	1.4±0.2	34	45±3.6	10
2by2-ANOVA:							
Group	*			*		*	
Treatment	*			*		ns	
Interaction	*			ns		ns	

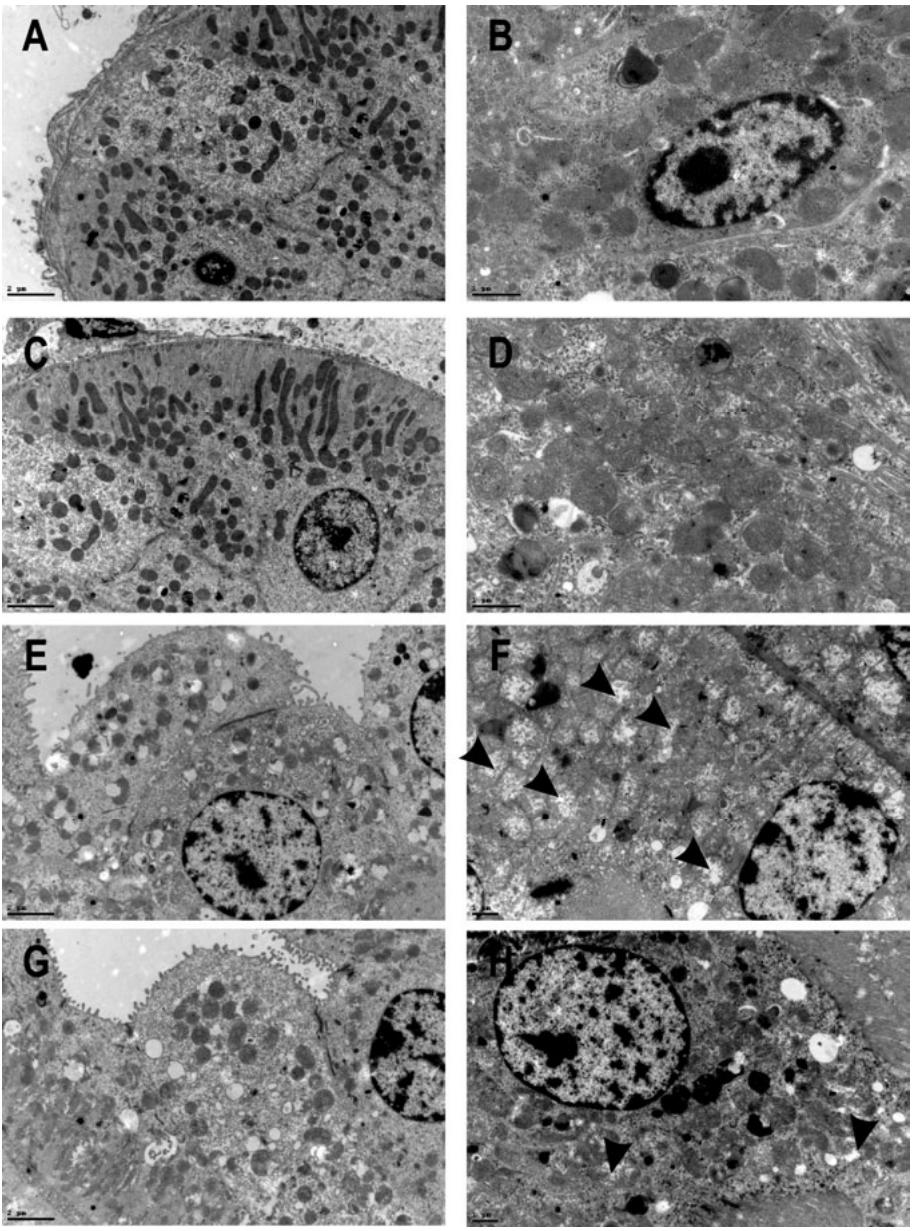

Figure 14. Representative electron micrographs from controls (A, B), controls + CoQ10 (C, D), db/db-mice (E, F) and db/db-mice + CoQ10 (G, H). Arrows indicate fragmented mitochondria.

Effects of Uncoupling Protein-2 knockdown (Study IV and V)

Administration of siRNA against UCP-2 resulted in approximately 30 and 50% knockdown of UCP-2 protein levels in control and diabetic animals, respectively (Fig 15). Increased level of UCP-2 together with increased glutamate-stimulated oxygen consumption was evident in untreated diabetic animals (Figs. 15 and 16). Control animals administered UCP-2 siRNA displayed increased glutamate-stimulated oxygen consumption. siRNA against UCP-2 resulted in further increased glutamate-stimulated oxygen consumption in diabetic animals. GDP inhibited the increased glutamate-stimulated oxygen consumption in untreated diabetic animals but not in control and diabetic animals treated with UCP-2 siRNA (Fig 16). Furthermore, ADP and CAT only affected oxygen consumption in mitochondria isolated from UCP-2 siRNA-treated animals (Figs. 17 and 18).

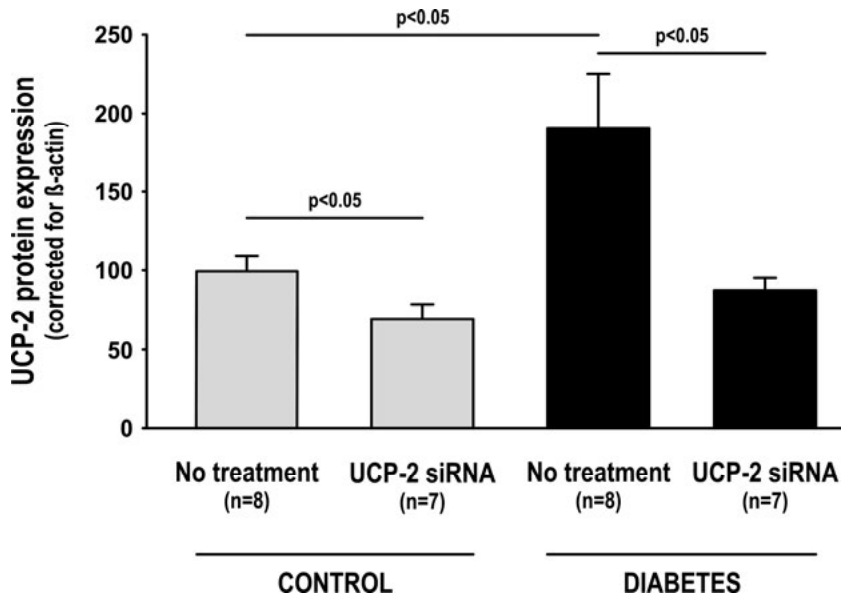

Figure 15. UCP-2 protein levels in control and diabetic rats with and without siRNA against UCP-2. All values are presented as mean±SEM.

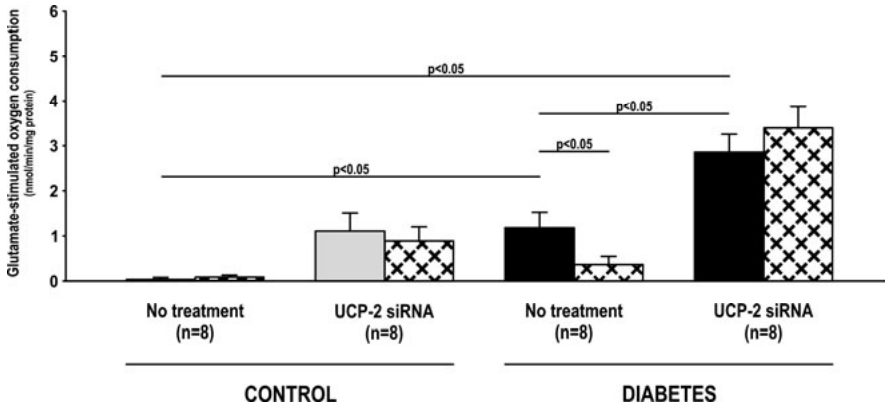

Figure 16. Glutamate-stimulated oxygen consumption during oligomycin (solid bars) and the effect of GDP (patterned bars) on kidney mitochondria isolated from control and diabetic rats with and without siRNA against UCP-2. All values are presented as mean±SEM.

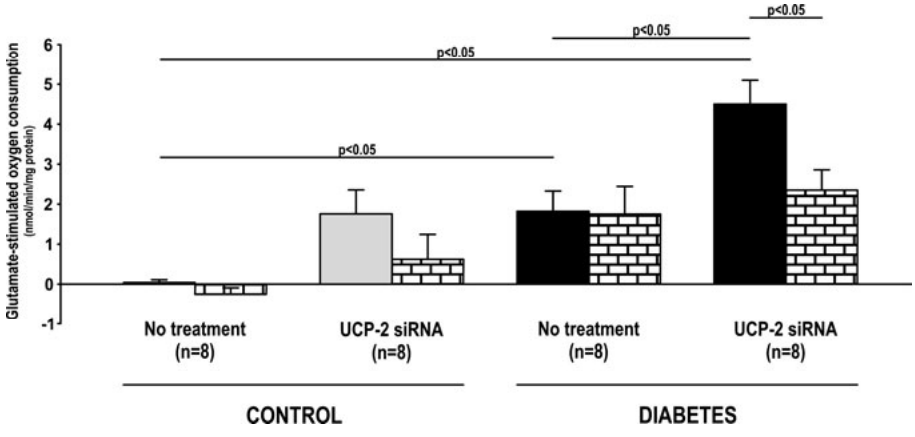

Figure 17. Glutamate-stimulated oxygen consumption during oligomycin (solid bars) and the effect of ADP (patterned bars) on kidney mitochondria isolated from control and diabetic rats with and without siRNA against UCP-2. All values are presented as mean±SEM.

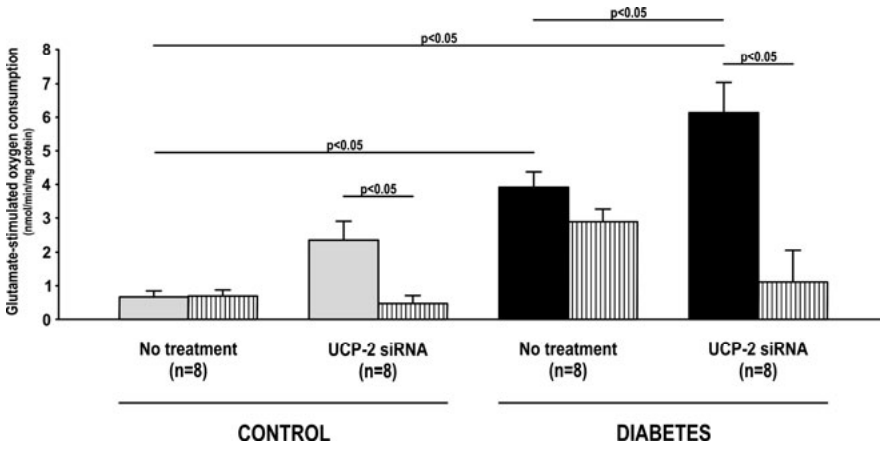

Figure 18. Glutamate-stimulated oxygen consumption during oligomycin (solid bars) and the effect of CAT (patterned bars) on kidney mitochondria isolated from control and diabetic rats with and without siRNA against UCP-2. All values are presented as mean±SEM.

Mitochondria membrane potential was unaltered in untreated diabetic animals, but reduced after UCP-2 siRNA. Administration of UCP-2 siRNA did not affect membrane potential in controls. GDP increased membrane potential in untreated diabetic animals but did not have an effect after siRNA against UCP-2 (Fig 19).

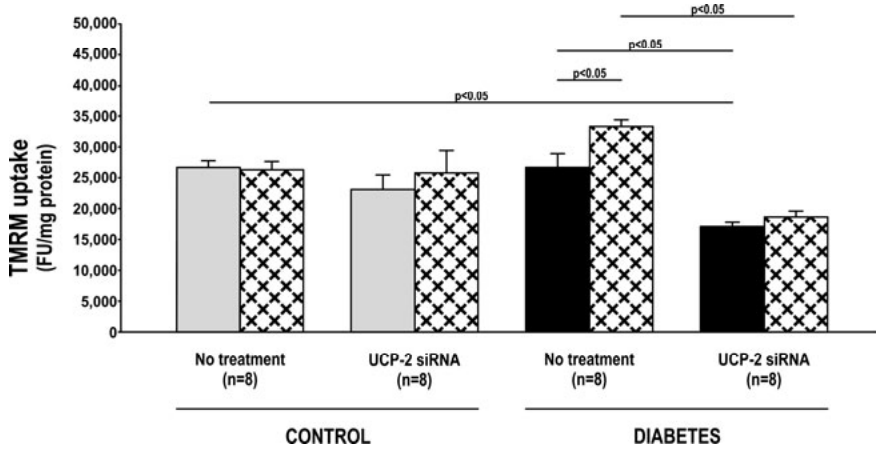

Figure 19. Tetramethyl rhodamine methylester (TMRM)-uptake during oligomycin (solid bars) and effect of GDP (patterned bars) in mitochondria isolated from control and diabetic rats with and without siRNA against UCP-2. All values are presented as mean±SEM.

Control and diabetic animals with siRNA against UCP-2 had similar levels of mitochondria ATP production. Mitochondria ATP production could be efficiently reduced by oligomycin or FCCP but was unaffected by CAT (Fig. 20).

Increased levels of TBARS in kidney cortex and MDA in plasma were observed in diabetic animals. UCP-2 siRNA reduced TBARS in diabetic animals but had no effect on plasma MDA. No effect of siRNA on TBARS and MDA levels was observed in control animals (Fig 21).

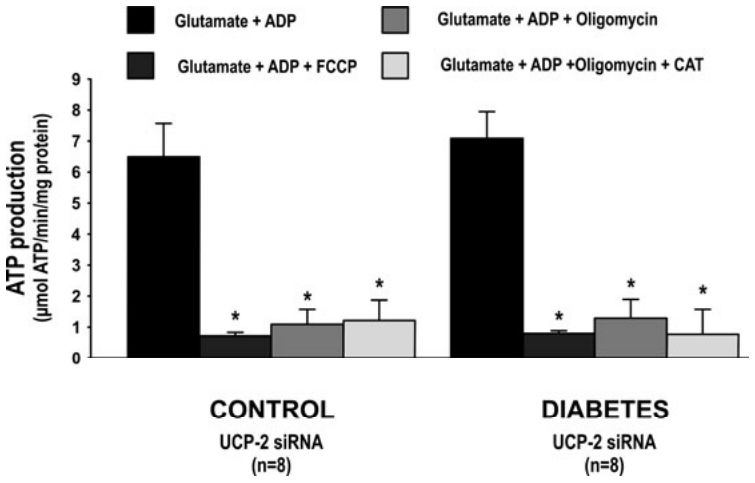

Figure 20. ATP production in kidney mitochondria isolated from control and diabetic rats with siRNA against UCP-2. All values are presented as mean±SEM. * denotes $p<0.05$ versus mitochondria with glutamate and ADP in each group.

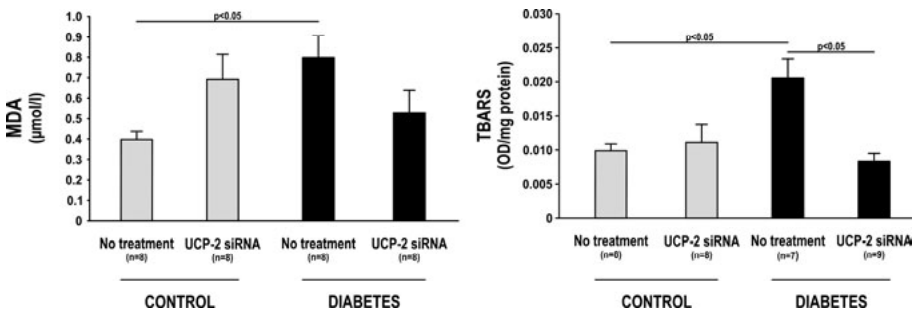

Figure 21. Malondialdehyde (MDA) levels in plasma (left) and thiobarbituric reactive substances (TBARS) levels in kidney cortex (right) in control and diabetic rats with and without siRNA against UCP-2. All values are presented as mean±SEM.

In vivo kidney function was also evaluated after siRNA against UCP-2. In this study, UCP-2 knockdown resulted in similar reduction of UCP-2 protein levels as in the study investigating mitochondria function (Fig. 15). Diabetic animals displayed glomerular hyperfiltration, increased renal blood flow, total kidney oxygen consumption and reduced kidney tissue oxygen tension and efficiency for tubular sodium transport. UCP-2 knockdown failed to affect any of the investigated parameters (Figs. 22-24). Scrambled siRNA did not affect any of the investigated parameters.

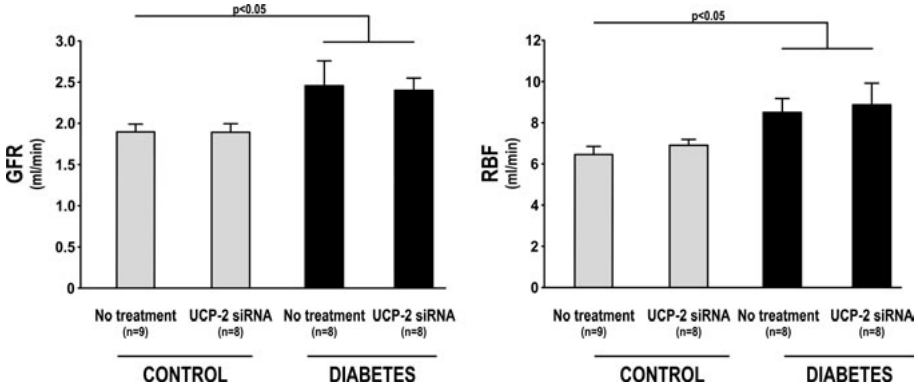

Figure 22. Glomerular filtration rate (GFR, left) and renal blood flow (RBF, right) in control and diabetic rats with and without siRNA against UCP-2. All values are presented as mean±SEM.

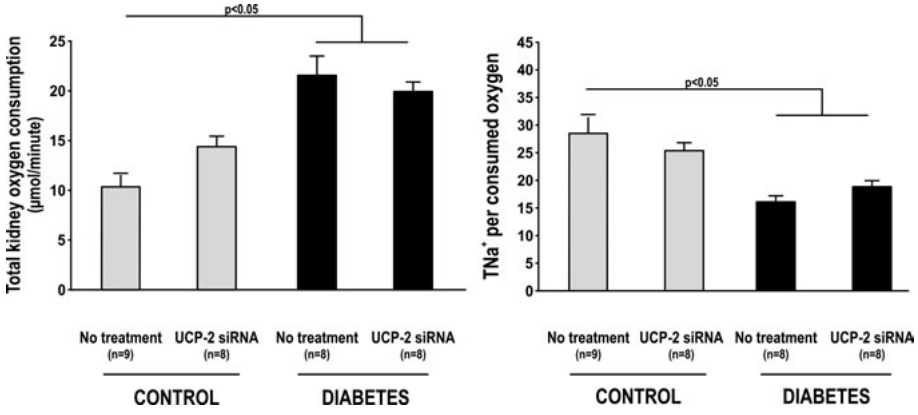

Figure 23. Total kidney oxygen consumption (left) and efficiency for tubular sodium transport (TNa^+ per consumed oxygen, right) in control and diabetic rats with and without siRNA against UCP-2. All values are presented as mean±SEM.

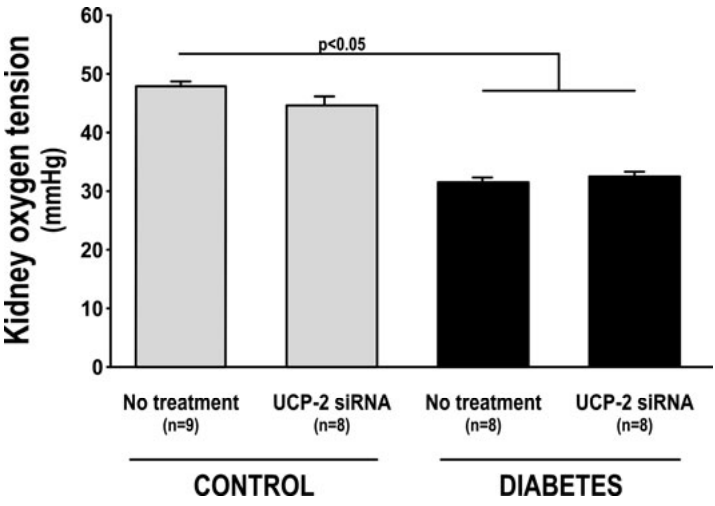

Figure 24. Kidney cortical tissue oxygen tension in control and diabetic rats with and without siRNA against UCP-2. All values are presented as mean±SEM.

Kidney function after increased mitochondria uncoupling (Study VI)

Treatment with the mitochondria uncoupler DNP did not affect body weights, blood glucose levels, kidney weight, mean arterial pressure, renal blood flow, GFR or sodium excretion but increased food/water intake and kidney oxygen delivery compared to control animals (Table 3). DNP-treated animals had increased hematocrit and hemoglobin compared to controls (Fig. 25). Also, DNP treatment increased total kidney oxygen consumption, reduced efficiency for tubular sodium transport (Fig. 26) and resulted in a decreased kidney cortical and medullary tissue oxygen tension (Fig. 27).

Table 3. Body weight (BW), blood glucose (BG), kidney weight (KW), food/water intake (food and water int.), mean arterial pressure (MAP), renal blood flow (RBF), glomerular filtration rate (GFR), kidney delivery of oxygen (DO_2) and excretion of sodium (Na^+_{excr}) in rats with and without DNP. * denotes $p<0.05$ compared to control animals, N=8-14 in each group.

	BW (g)	BG (mmol/l)	KW (g)	Food int. (g/day)	Water int. (ml/day)	MAP (mmHg)	RBF (ml/min)	GFR (ml/min)	DO_2 (µmol/ml/min)	Na_{excr} (µmol/min)
Control	433±21	6.1±0.4	1.3±0.0	24±1	31±1	101±3	10.3±4	1.5±0.1	1775±71	0.1±0.1
DNP	452±13	5.4±0.4	1.4±0.0	29±1*	40±1*	94±9	9.1±0.7	1.3±0.1	2124±58	0.1±0.1

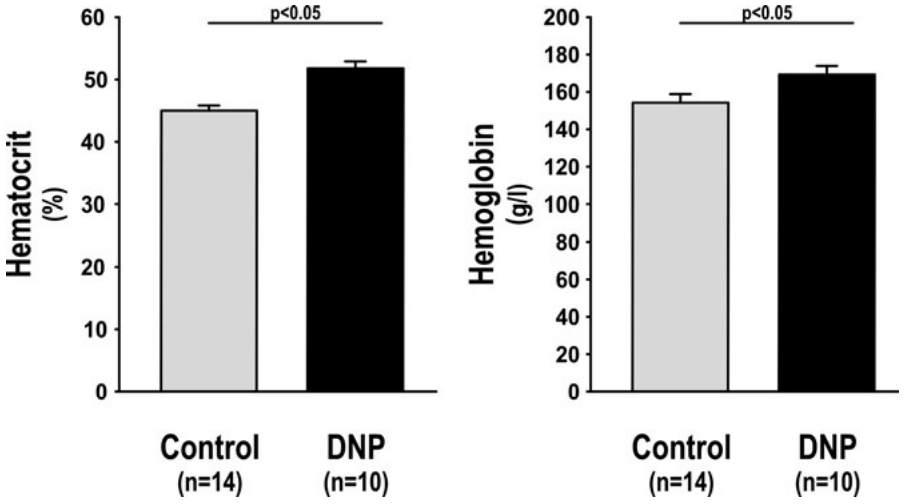

Figure 25. Hematocrit (left) and hemoglobin (right) in normoglycemic rats with and without DNP. All values are presented as mean±SEM.

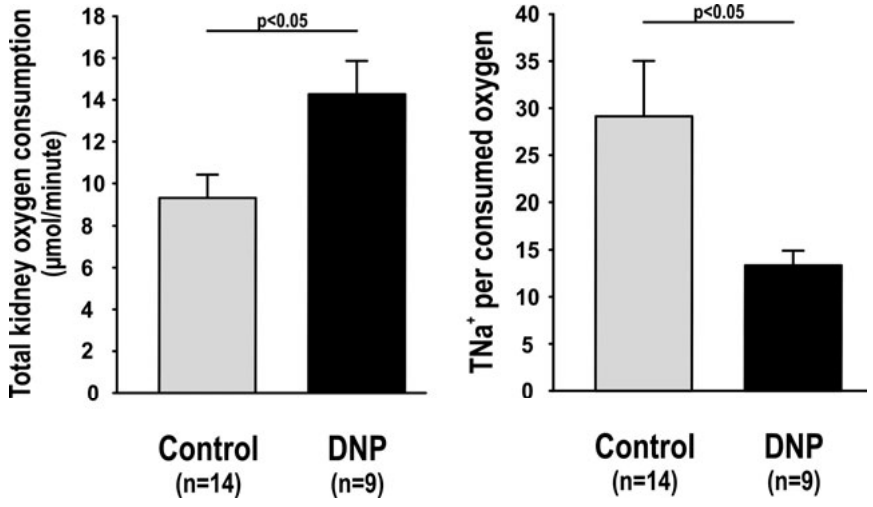

Figure 26. Total kidney oxygen consumption (left) and efficiency for tubular sodium transport (TNa^+ per consumed oxygen, right) in normoglycemic rats with and without DNP. All values are presented as mean±SEM.

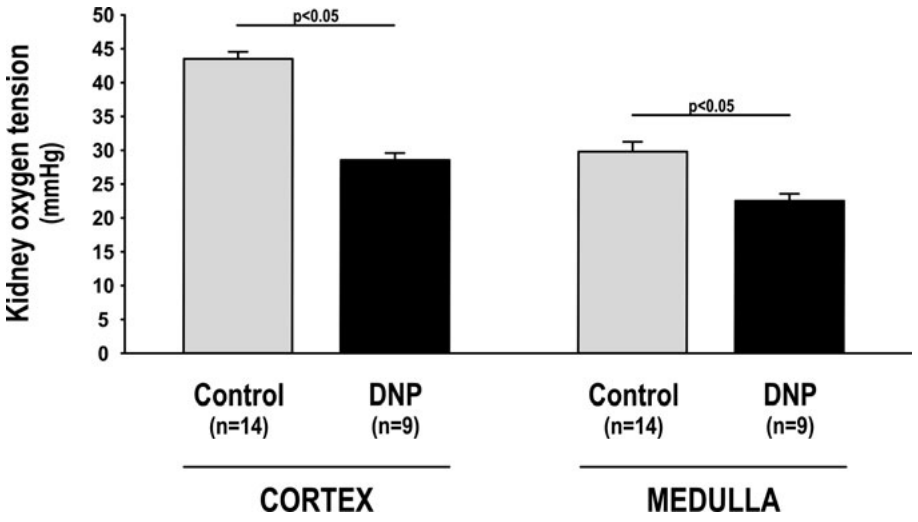

Figure 27. Kidney oxygen tension in cortex and medulla of normoglycemic rats with and without DNP. All values are presented as mean±SEM.

Increased protein excretion and staining of vimentin and ED-1 was observed after DNP-treatment (Fig. 28, 29 and 30). Acute infusion of DNP in vehicle-treated controls resulted in decreased cortical and medullary oxygen tension (34±2 vs. 44±1 mmHg and 26±1 vs. 30±2 mmHg; both $p<0.05$) but did not result in proteinuria (46.9±7.7 vs. 50.9±5.9 µg/minute; ns). Hypoxia inducible factor (HIF)-1α was increased after DNP but erythropoietin, glucose transporter-1, vascular endothelial growth factor, and heme oxygenase-1 remained unaffected (Table 4).

Table 4. mRNA levels of HIF-1α and HIF-responsive genes in rats with and without DNP. HO-1 – heme oxygenase 1, VEGF – vascular endothelial growth factor, GLUT – glucose transporter 1, EPO – erythropoietin. Values are standardized to controls, * denotes $p<0.05$ compared to control animals, N=6-8 in each group.

	HIF-1α	HO-1	EPO	GLUT-1	VEGF
Control	1.0±0.3	1.0±.4	1.0±0.4	1.0±0.2	1.0±0.3
DNP	3.2±0.8*	4.2±0.1*	1.1±0.4	0.7±0.3	0.7±0.3

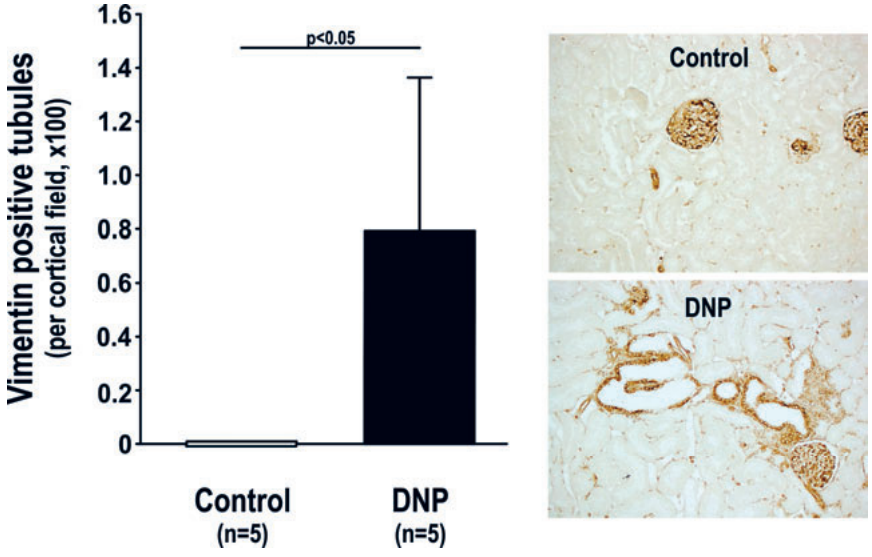

Figure 28. Vimentin staining in kidneys from normoglycemic rats with and without DNP. All values are presented as mean±SEM.

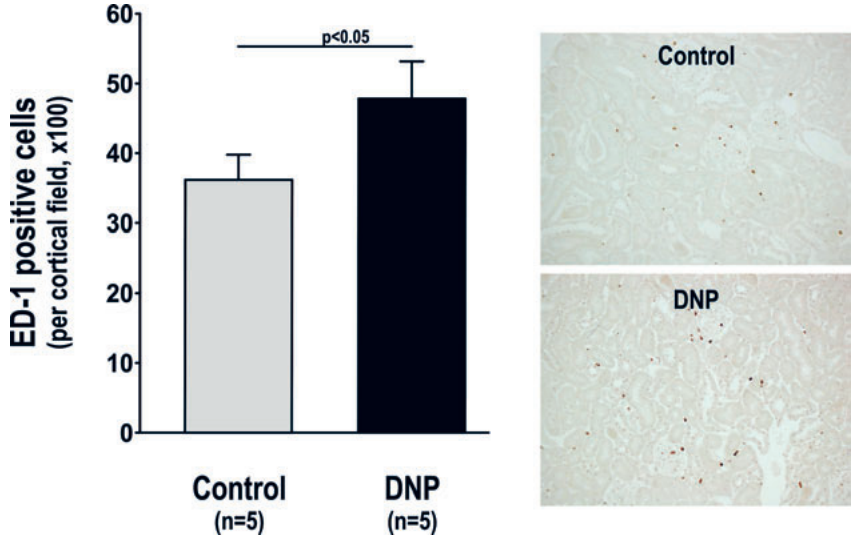

Figure 29. Infiltration of ED-1 positive cells in kidneys from normoglycemic rats with and without DNP. All values are presented as mean±SEM.

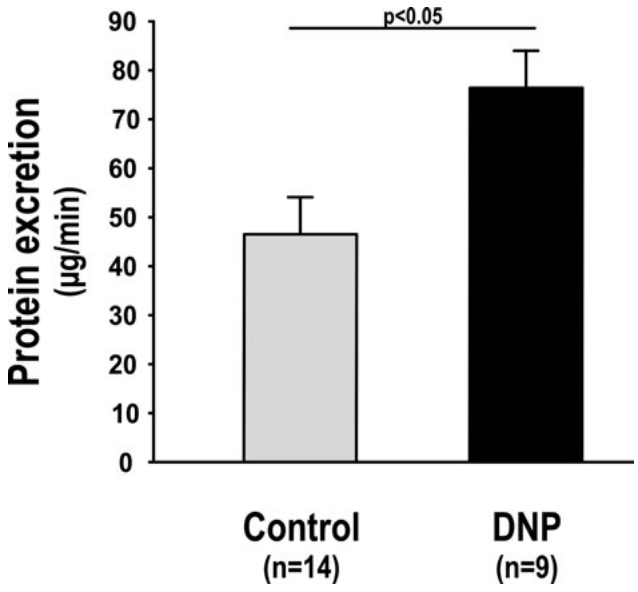

Figure 30. Urinary protein excretion in normoglycemic rats with and without DNP. All values are presented as mean±SEM.

"It is impossible to thoroughly enjoy idling unless one has plenty of work to do. " *JK Jerome (1859-1927)*

Discussion

UCP-2 was the only isoform detected in the kidney and localized to the proximal tubule and mTAL segments. Several others have corroborated the localization of UCP-2 in human, rat and mice kidneys [80-82]. The immunohistochemical results do not exclude UCP-2 from being expressed at low levels in other tubular segments, but since the proximal tubule and mTAL perform a majority of the tubular electrolyte transport these cells have a high mitochondria content, which facilitates the detection of mitochondrial proteins.

Proximal tubular cells from diabetic animals had increased transport-independent oxygen consumption, indicating increased basal metabolism. Indeed, this was correlated to increased protein levels of UCP-2. Isolated mitochondria from diabetic animals displayed increased glutamate-stimulated oxygen consumption, demonstrating mitochondria uncoupling. Furthermore, the uncoupling was inhibited by removing the fatty acids, which further supports the proposed mechanism of UCP-2 as a fatty acid cycler. Finally, the uncoupling was also inhibited by GDP, a known inhibitor of UCP activity [77, 88, 107, 139]. In essence, we demonstrated diabetes-induced mitochondria uncoupling via UCP-2.

For several years after the discovery of UCP-2 and-3, it was debated whether these two isoforms of UCP were true uncouplers of mitochondrial respiration. The literature in regard to biochemical investigations is conflicting. UCP-2 and -3 investigated under different conditions resulted in different conclusions [80, 99, 140, 141]. However, it is possible that mechanisms of activating UCP-2 and -3 *in vitro* are different or differently regulated compared to the *in vivo* situation. Indeed, UCP-2 was detected in kidneys from normoglycemic controls but did not cause mitochondria uncoupling even after addition of fatty acids, which are known activators of UCPs *in vitro*. Similarly, in study III there was no uncoupling detected in control mice despite a clear presence of UCP-2 protein. Importantly, it has been reported that UCP-2 and -3 can play a role during disease states in various tissues [142-145]. Insulin treatment to diabetic animals resulted in decreased UCP-2 protein levels, correlating with normalized transport-independent oxygen consumption in proximal tubular cells. Therefore, activation of UCP-2 in diabetic animals is clearly connected to the level of hyperglycemia and also excludes streptozotocin as having any effect on UCP-2 function.

Hyperglycemia is closely associated with oxidative stress and, indeed, oxidative stress is a known activator of UCPs although there are conflicting results in the literature. Echtay *et al.* demonstrated by increasing the level of $O_2^{\bullet-}$ and measuring mitochondria uncoupling simultaneously that UCPs could be activated by $O_2^{\bullet-}$ [89]. However, this study was later questioned by Couplan *et al*. [146]. A following study by Echtay *et al.*, claiming to have taken the arguments of Couplan *et al.* into account once again demonstrated $O_2^{\bullet-}$-induced mitochondria uncoupling [105]. Importantly, it was reported by another group that kidney mitochondria from UCP-2-deficient mice lacked $O_2^{\bullet-}$-inducible uncoupling. Furthermore, uncoupling could be reduced in mitochondria from wild-type mice but not from UCP-2-deficient mice [107]. The available literature is predominantly in favor of UCPs being activated by oxidative stress and this is further solidified from the present results in which GDP-sensitive uncoupling was observed in db/db-mice. It should be noted that this was not associated with increased UCP-2 protein levels but instead correlated with increased oxidative stress, manifested as protein carbonylation. CoQ10 is our only lipid-soluble endogenous antioxidant and a part of the ETC [147, 148]. Mutations of genes regulating CoQ10 synthesis results in primary nephropathy [149]. Importantly, treatment with the antioxidant CoQ10 reduced oxidative stress, prevented mitochondria uncoupling and decreased UCP-2 protein levels. Lipid peroxidation products can activate GDP-sensitive mitochondria uncoupling [104] and db/db-mice exhibit dyslipidemia [56, 128]. Whether activation of UCP-2 in our model occurs via lipid peroxidation products, directly from mitochondria derived $O_2^{\bullet-}$ or other unknown oxidative stress-related factors cannot be determined from the present results. However, results from the db/db-mice and insulin treated diabetic rats are in favor of hyperglycemia-mediated oxidative stress being a crucial inducer of mitochondria uncoupling via UCP-2.

The fact that UCP-2 is upregulated in type 1 diabetic rat kidneys but activated in type 2 diabetic mouse kidneys may of course be related to species differences. However, it may also reflect differences in the time-course of blood glucose increase as streptozotocin increases blood glucose levels rapidly over 24 hours but db/db-mice have slowly increasing blood glucose levels over several weeks. Clearly, this interesting difference warrants further investigation.

Mitochondria morphology alterations are known to contribute to hyperglycemia-induced $O_2^{\bullet-}$ production [150]. Kidney mitochondria from db/db-mice were larger and more fragmented compared to mitochondria from corresponding wild-type mice. Increased fragmentation is likely to contribute to increased the $O_2^{\bullet-}$ formation and, indeed, db/db-mice had increased protein carbonyls in kidney cortex. The increased cellular content of mitochondria in db/db-mice possibly reflects a cellular response to increased substrate load due to hyperglycemia since CoQ10 did not affect either blood glucose levels or cellular mitochondria content in these animals.

Importantly, db/db-mice presented with glomerular hyperfiltration and proteinuria, both known as clinical features of diabetic nephropathy and predictors of progression to ESRD [32, 34, 36, 151]. Increased proteinuria predicts a more rapid loss of GFR and is therefore considered a very good independent predictor of disease progression [35]. In summary, db/db-mice exhibited mitochondria uncoupling, altered mitochondria morphology and clinical features of diabetic nephropathy, all of which were prevented by CoQ10. These results demonstrate that oxidative stress-induced mitochondria uncoupling indeed can play an important role in the development of diabetic nephropathy.

Clearly, UCP-2 plays a role in diabetic kidneys and an obvious question was whether reduced levels of UCP-2 in diabetic kidneys would affect mitochondria and/or kidney function. By administering siRNA to rats we successfully reduced UCP-2 proteins levels by approximately 30 and 50% in control and diabetic animals, respectively. Paradoxically, knockdown of UCP-2 resulted in increased mitochondria uncoupling, manifested as increased glutamate-stimulated oxygen consumption. We observed this in both control and diabetic animals, and it was especially surprising in controls since UCP-2 does not perform an uncoupling function in these animals. However, it appears that the presence of UCP-2 in the inner membrane is important enough to be replaced by other mechanisms when its expression is reduced by the siRNA knockdown. We postulate that knockdown of UCP-2 results in an initially increased oxidative stress, in accordance with other reports [76, 100], leading to activation of secondary mitochondria uncoupling mechanisms in order to protect mitochondria from devastating oxidative stress. The resulting mitochondria uncoupling in the siRNA-treated animals was insensitive to GDP, but was inhibited by ADP. These results are somewhat surprising since all purine nucleotides are known as UCP-inhibitors [77, 88]. The effect of purine nucleotide on the function of UCPs has been studied mainly *in vitro* during control conditions and there is a lack of studies using mitochondria from pathological conditions, such as diabetes. Also, in study II, the increased uncoupling in diabetic animals was not inhibited by addition of ADP during ATP-synthase inhibition. Therefore, the role of ADP in UCP-2 inhibition needs further investigation, preferably during hyperglycemic conditions where UCPs are activated *in vivo*.

The observation that ADP inhibited mitochondria uncoupling suggested involvement of the ANT, a translocater of ADP and ATP during normal conditions. However, ANT is a known mitochondria uncoupler under certain conditions [11]. When adding ADP without matched amounts of ATP i.e. in the presence of oligomycin, ANT closes in c-conformation and does not perform nucleotide translocation, and, as observed in mitochondria from siRNA-treated animals, it does not perform mitochondria uncoupling. This suggests that ANT is performing nucleotide translocation and mitochondria uncoupling simultaneously when matched amount of ADP and ATP are

present. Indeed, mitochondria ATP production was not absent during ATP-synthase inhibition. Koulintchenko *et al.* reported that DNA-import via the ANT in potato tuber mitochondria was inhibited by ADP only in the presence of oligomycin [152], which strengthens the theory that ANT performs translocation in the presence of oligomycin in our experimental setting. Importantly, locking the ANT in c-conformation by addition of CAT inhibited both DNA import [152] and mitochondria uncoupling in our experiments. This demonstrates an important role of ANT in the absence of normal UCP-2 function. Furthermore, skeletal muscle mitochondria displayed increased CAT-sensitive uncoupling in UCP-2 deficient mice subjected to caloric restriction and it was suggested that ANT-mediated uncoupling compensated for the lack of UCP-2 during situations of metabolic stress [153].

Mitochondria membrane potential was not increased in untreated diabetic animals. This is in contrast to studies performed in cultured cells were hyperglycemic conditions commonly results in increased membrane potential [49, 67, 69]. In studies performed on cultured cells the mitochondria are subjected to increased substrate load to the ETC due to the hyperglycemia. However, isolated mitochondria from diabetic animals are subjected to the same substrate load as control mitochondria. Furthermore, activation of UCP-2 *in vivo* decreases membrane potential and any differences will be difficult to observe *in vitro*. GDP increased the membrane potential in mitochondria from untreated diabetic animals, demonstrating that the membrane potential indeed is elevated in the absence of mitochondria uncoupling and that UCP-2-mediated uncoupling is a potent regulator of mitochondria membrane potential. Importantly, increased mitochondria uncoupling in siRNA-treated diabetic animals decreased the membrane potential and it was no longer altered by GDP. The increased mitochondria uncoupling in siRNA-treated diabetic animals also normalized kidney TBARS levels, demonstrating that increased mitochondria uncoupling has the potential to regulate whole-organ oxidative stress. Plasma MDA level also increased with diabetes but was not affected by UCP-2 siRNA, probably because plasma MDA levels reflect oxidative stress status in the whole body. It should be noted that since we only reduced UCP-2 expression and that isoform is highly expressed in kidney tissue, it is possible that the main effect is confined to the kidneys.

Untreated diabetic animals displayed altered kidney function in terms of glomerular hyperfiltration, increased renal blood flow and total kidney oxygen consumption, decreased kidney tissue oxygen tension and efficiency for tubular sodium transport. However, despite 50% knockdown of UCP-2, none of these parameters were affected. Possible reasons include that only a partial knockdown of UCP-2 was achieved, that a too short duration occurred between siRNA-administration and measurements of kidney function, and the fact that the knockdown of UCP-2 caused a compensatory increase of ANT-mediated uncoupling. Further studies are in progress, using UCP-2

deficient mice which allows for long-term studies of the specific role of UCP-2 for kidney function during diabetes.

Controlling the level of oxidative stress is clearly beneficial in experimental models of diabetes [52-54, 66] and patients with stricter glycemic control have reduced severity of diabetic complications [43]. However, mitochondria uncoupling in the kidney may not be the best oxidant defense system. As discussed in the introduction, the kidney tissue oxygen tension is low already during normal conditions due to the presence of a diffusion shunt elegantly demonstrated by Levy *et al.* [7, 8]. Supersaturated oxygen buffer containing fluorescent erythrocytes was injected into the renal artery and the transit time of the labeled erythrocytes versus the oxygen peak to appear in the renal vein were studied. It was demonstrated that the oxygen peak appeared in average 1.25 s earlier than the erythrocytes. Erythrocytes are restricted to the vasculature whereas dissolved oxygen can utilize a morphological arterio-venous countercurrent to travel a shorter distance, and thus appear in the renal vein before the arrival of erythrocytes. This study was the first to demonstrate the presence of an intrarenal functional diffusion shunt of oxygen. It should also be considered that increased renal blood flow is likely to increase the tubular load of electrolytes due to increased GFR and therefore increase the metabolic demand. Consequently, increased kidney oxygen metabolism is likely to initiate kidney tissue hypoxia resulting in kidney damage. Hyperglycemia-induced mitochondria uncoupling may therefore be a contributor to the development of diabetic nephropathy although it may protect against oxidative stress.

Several studies have established decreased kidney tissue oxygen tension in diabetes, both in animals [53, 54, 109-112] and patients [113]. However, the role of decreased tissue oxygen tension for the development of diabetic nephropathy is difficult to distinguish from concomitantly occurring effects of hyperglycemia and oxidative stress and we opted to clarify this by administration of DNP to healthy rats. DNP is a chemical uncoupler of mitochondria and due to its ability to increase metabolism DNP was popular as a diet pill in the early 1930's. However, DNP have a very narrow therapeutic window in humans, so overdose-induced fatalities were common [154] and DNP was rapidly banned from the market after the reports of 175 cases of cataract in the period of a couple of months [155].

DNP is well known to increase oxygen consumption and reduce oxidative stress in animals [156]. Our results demonstrate that administration of DNP to healthy rats for 30 days increased total kidney oxygen consumption and resulted in decreased kidney tissue oxygen tension. DNP did not affect blood glucose in these animals, and we therefore concluded that we established a model of decreased kidney tissue oxygen tension independently of hyperglycemia and oxidative stress. Importantly, DNP-administration caused proteinuria and increased staining of vimentin, a marker of tubular injury [157, 158], and infiltration ED-1 positive immune cells. It is known that long-term

administration of DNP results in proteinuria both in animals and patients [159-161] and proteinuria may aggravate kidney injury by inducing inflammation and apoptosis in proximal tubular cells [162, 163]. DNP-treated animals had increased hematocrit to unchanged renal blood flow, resulting in increased renal delivery of oxygen. However, this did not affect kidney tissue oxygen tension. This may be due to concomitantly increased renal metabolism that will increase arterio-venous shunting of oxygen caused by the lower oxygen content in the venous blood.

The HIF-system is an important mechanism to counteract sustained hypoxia [164, 165]. Transcriptionally active HIF consists of two subunits; the rapidly degraded α-subunit and the constitutively expressed β-subunit. Prolyl hydroxylases control hydroxylation of the α-subunit and thereby recognition by the von Hippel Lindau protein, subsequent ubiquitinylation and degradation. As prolyl hydroxylases require oxygen the α-subunit escapes degradation under hypoxia, ultimately resulting in transcription of genes controlling, among others, angiogenesis, anaerobic metabolism, delivery of oxygen and antioxidative mechanisms [164, 165]. Indeed, HIF-1α mRNA increased after DNP-administration, in agreement with a previous report [166]. Increased hematocrit could not be attributed to increased transcription of erythropoietin in the kidney. This is seemingly contradictory in the view of increased hematocrit but it should be noted that circulating erythropoietin levels are regulated also by other tissues than the kidney [167].

Nephrotoxicity of DNP *per se* is hard to exclude as other chemical uncouplers such as FCCP have similar chemical structure and therefore is likely to have similar toxicity. However, acute administration of DNP to healthy rats decreased kidney tissue oxygen tension but did not result in proteinuria. Also, it is unlikely that kidney injury after DNP is due to ATP-depletion as both groups exhibited similar GFR and sodium excretion which is in accordance with other studies [168, 169]. In summary, no acute toxicity of DNP could be determined. However, DNP is indeed nephrotoxic, but the mechanism might very well involve increased kidney oxygen consumption resulting in kidney hypoxia.

In 1998 it was proposed by Fine *et al.* that kidney hypoxia may be a unifying pathway to kidney damage [114] and chronic tubulointerstitial hypoxia is now acknowledged as a common pathway to kidney damage and ERSD [116-120]. Interestingly, high altitude *per se* increased the prevalence of age-adjusted non-diabetic ESRD in Navajo Indians by 1.8-fold [170]. Furthermore, type 2 diabetic patients living at 1700 m above sea level had increased prevalence of proteinuria compared to a matching patient population living at sea level. Importantly, there were no differences between patient populations in mean arterial pressure, lipidemia status, glycemic control and prevalence of retinopathy [171].

By affecting kidney tissue oxygen tension hyperglycemia-induced mitochondria uncoupling via UCP-2 has the potential to mediate kidney damage

and may therefore play a pivotal role in the development of diabetic nephropathy.

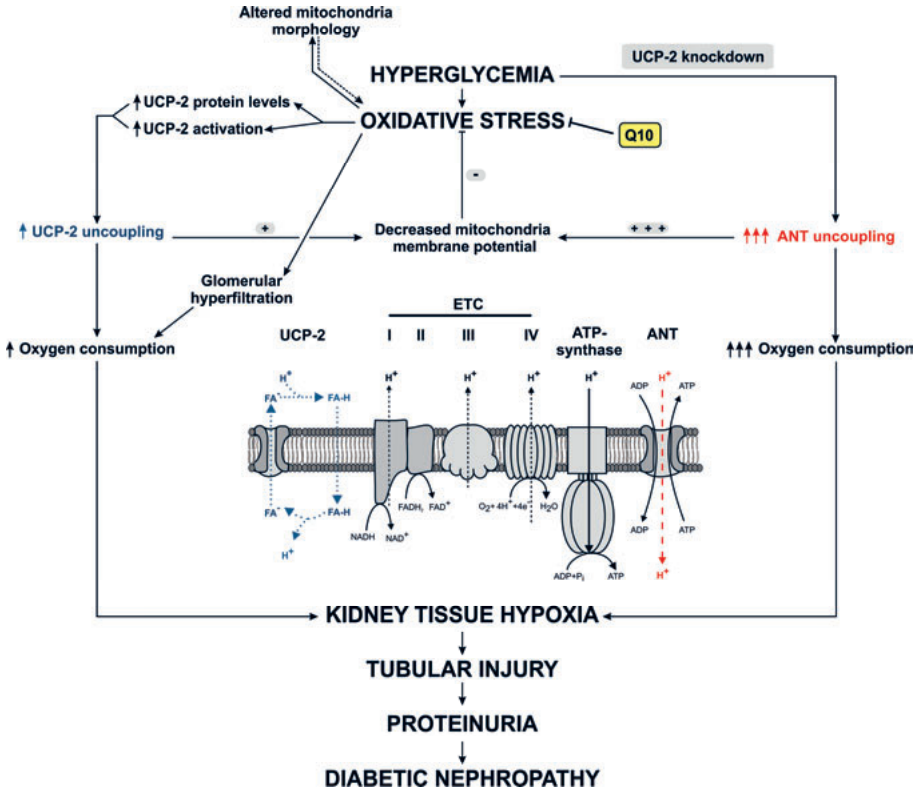

Figure 31. The unified mechanism for development of diabetic nephropathy presented in this thesis. Displayed in the middle is the mitochondria electron transport chain (ETC) with the function of uncoupling protein-2 (UCP-2) on the left in blue and the proposed uncoupling via the adenosine nucleotide transporter (ANT) after siRNA against UCP-2 on the right in red. ADP – adenosine diphosphate, ATP – adenosine triphosphate transporter, FA^- – charged fatty acid, $FADH_2$ – reduced 1,5-dihydro-flavin adenine dinucleotide, FA-H – protonated fatty acid, H^+ – proton, NADH – reduced nicotineamide adenine dinucleotide, Pi – inorganic phosphate, Q10 - coenzyme Q10

Conclusions

The results from the studies included in this thesis demonstrate that increased mitochondria uncoupling in diabetic kidneys contributes to the development of diabetic nephropathy. Specifically, it is concluded that:

- Hyperglycemia-induced oxidative stress results in mitochondria uncoupling via UCP-2 in kidneys from type 1 and type 2 diabetic animal models.

- Increased mitochondria uncoupling has the potential to regulate mitochondria membrane potential and oxidative stress in the kidney.

- The importance of UCP-2 and its uncoupling function for normal kidney mitochondria function is demonstrated by the rapid replacement by the adenosine nucleotide transporter if normal UCP-2 function acutely is reduced.

- Increased mitochondria oxygen consumption causes kidney tissue hypoxia and mediates kidney damage independently of hyperglycemia and oxidative stress.

Populärvetenskaplig sammanfattning

Inledning

Njurskador till följd av diabetes, så kallad diabetesnefropati, drabbar en tredjedel av patienter med diabetes och leder till kronisk njursvikt med behov av dialys eller transplantation av njuren som följd. Njurskador drabbar både personer med typ 1 diabetes såväl som typ-2 diabetes. Typ 1 diabetes beror på en avsaknad av insulin (hormonet som sänker nivån av socker i blodet) och kallas ofta ungdomsdiabetes då sjukdomen debuterar i unga år. Typ 2 diabetes beror på att insulinet finns men inte fungerar, så kallad insulin resistens. Denna sjukdom uppkommer ofta i äldre och i samband med övervikt. Mekanismerna bakom utvecklandet av diabetesnefropati är inte klarlagda men forskning visar att tidiga mekanismer som involverar oxidativ stress och en förändrad hantering av syrgas i njuren är starkt bidragande. Oxidativ stress är det sammantagna namnet för de skador på DNA, proteiner och cellmembran som orsakas av fria syreradikaler. För hög oxidativ stress kommer till slut att leda till cell och vävnadsdöd.

Mitokondrien är cellens energifabriker och därmed livsviktiga för cellens överlevnad men märkligt nog är mitokondrien även en stor källa till oxidativ stress. I mitokondrien finns fyra komplex som tillsammans kallas för mitokondriens elektrontransportkedja. Elektroner transporteras från komplex ett och två till komplex fyra där elektronerna används för att förbruka syrgas. Denna transport av elektroner och konsumtion av syrgas är kopplat till en utförsel av vätejoner till utrymmet mellan mitokondriens två membraner. Då vätejonerna är laddade skapar ansamlingen en membranpotential som det ATP-producerande enzymet sedan utnyttjar för att få tillräcklig energi att skapa cellens energimolekyl; ATP (Figur 32, steg 1-4).

Från komplex ett och tre kan det hända att elektroner ”lossnar” från transportprocessen och istället hoppar direkt till syrgas, vilket då bildar en fri syreradikal. Det är känt att mitokondrier bildar fria syreradikaler under normala förhållanden men till en väldigt låg grad. Risken finns dock att en ökad produktion av fria syreradikaler leder till en ond cirkel där skadade mitokondrier bildar mer fria syreradikaler, skadas ännu mer och därmed ökar produktionen av fria syreradikaler ytterligare.

Det är känt att diabetiska mitokondrier ökar produktionen av fria syreradikaler markant vilket beror på att de har en högre membranpotential än icke-diabetiska mitokondrier. En skyddande mekanism mot detta är fenome-

net mitokondriell frikoppling vilket utförs av så kallade ”frikopplande proteiner” (uncoupling proteins, UCPs). UCP släpper ner vätejoner över mitokondriens inre membran vilket sänker membranpotentialen och därmed också minskar produktionen av fria syreradikaler. Mitokondriell frikoppling har dock en potentiellt skadlig sidoeffekt; en ökad syrgaskonsumtion som kan vara skadande för njuren eftersom det kan leda till syrgasbrist (Figur 32, steg 5-7).

Njuren har normalt en låg mängd syrgas i vävnaden trots en bra blodförsörjning. Njuren kan inte heller kompensera en syrgasbrist med ett ökat blodflöde eftersom detta även ger en ökad filtration i njuren. Därmed ökar njurens energikrävande arbete vilket gör att syrgaskonsumtionen ökar och den positiva effekten uteblir.

Mitokondriell frikoppling kan därmed vara bra på grund av att den oxidativa stressen minskar men samtidigt kan det alltså vara skadligt för njuren eftersom syrgaskonsumtionen ökar. Mitokondriell frikoppling har setts i hjärtmuskulaturen hos diabetiska patienter men rollen i njuren har ännu inte undersökts. Därför fokuserar denna avhandling på rollen av mitokondriell frikoppling i utvecklandet av diabetesnefropati.

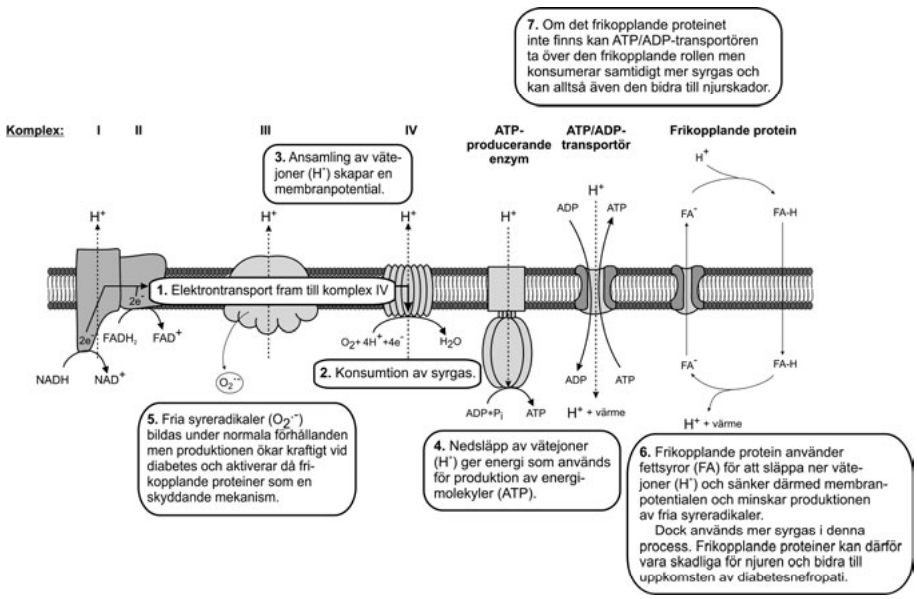

Figur 32. Sammanfattning av mitokondriens funktion under normala och diabetiska förhållanden samt rollen av frikopplande proteiner. ADP – adenosin difosfat, ATP – adenosin trifosfat, e^- – fri elektron, FA^- – laddad fetttsyra som ej kan passera membranet utan hjälp av frikopplande proteiner, FA-H – oladdad fettsyra som kan passera membranet, H^+ – vätejon, H_2O – vatten, NADH och $FADH_2$ – substrat som donerar elektroner till ETC, $O_2^{\bullet-}$ – fri syreradikal, Pi – inorganiskt fosfat. Modifierad från [74].

Resultat

I studie 1 var målet att identifiera vilka former av UCP som finns i njuren. Resultaten visade att UCP-2 var den enda formen av UCP i njuren och var lokaliserat till de delar som gör huvuddelen av njurens transportarbete och därmed också har mest mitokondrier. Diabetiska råttor visade ökade proteinnivåer av UCP-2 och vi såg även en ökad färgning av UCP-2 på vävnadssnitt jämfört med friska djur. Vidare i studie 2 såg vi återigen ökade nivåer av UCP-2 hos diabetiska råttor och nu undersökte vi även mitokondriens funktion. Den ökade nivån av UCP-2 orsakade mitokondriell frikoppling med ökad syrgaskonsumtion som följd. Det var viktigt att den ökade syrgaskonsumtionen kunde blockeras med guanosindifosfat (GDP), eftersom det är en specifik hämmare av UCP och således visar att det verkligen var UCP-2 som orsakade frikopplingen och inte någon annan mekanism.

Då vi i studie 2 valt att använda en typ 1 modell för diabetes valde vi i studie 3 att undersöka ifall samma mekanism för mitokondriell frikoppling fanns i njurarna hos en typ 2 diabetes modell; db/db-möss. Dessa möss saknar mekanismen som signalerar mättnad och forsätter istället att äta och öka i vikt tills de så småningom utvecklar typ 2 diabetes. I mitokondrier isolerade från njuren fann vi en frikoppling som var känslig för GDP men inte den ökade nivån av UCP-2 som vi fann i typ 1 diabetiska råttor (studie 2). Behandling med antioxidanten Q10 tog bort frikopplingen och vi kom då fram till slutsatsen att det var en aktivering av UCP-2 via oxidativ stress som orsakade mitokondriell frikoppling. Blockering av den mitokondriella frikopplingen med Q10 förhindrade uppkomsten av glomerulär hyperfiltration (en ökad hastighet i njurens filtration) och en ökad utsöndring av proteiner i urinen. Både hyperfiltration och proteinutsöndring är kända symptom på etablerade njurskador vilket visar att Q10 förhindrade uppkomsten av diabetesnefropati genom att förhindra mitokondriell frikoppling.

Studie 1-3 visade att diabetes och oxidativ stress orsakar en mitokondriell frikoppling i njuren via UCP-2 och i studie 4 ville vi närmare undersöka hur viktig denna frikoppling egentligen var. Genom att ge små interfererande RNA-molekyler (siRNA) kunde vi specifikt minska proteinnivån av UCP-2 med 30-50 %. Förvånande nog såg vi en ökad frikoppling i både friska och diabetiska djur istället för minskad frikoppling vilket vi hade förväntat oss. Vidare undersökning visade att när UCP-2 inte finns i tillräcklig mängd tar ATP/ADP-transportören i mitokondrien över rollen som frikopplare. Detta sänkte mitokondriens membranpotential och minskade även nivån av oxidativ stress i njuren. Alltså är mitokondriell frikoppling via UCP-2 en så pass viktig mekanism att om den sätts ur spel sker en kompensatorisk frikoppling via ATP/ADP-transportören. Nackdelen med denna kompensatoriska mekanism är att den använder ännu mer syrgas än UCP-2 och kan därför potentiellt vara mer skadande för njuren eftersom den borde resultera i en kraftigare syrgasbrist.

Vi mätte även njurfunktionen på råttor två dagar efter att vi gett siRNA mot UCP-2 i studie 5. Obehandlade diabetiska råttor hade ökad UCP-2 proteinnivå, en minskad mängd syrgas i njuren och även en minskad effektivitet för transport av salt i njuren men en minskning av UCP-2 nivån med 50 % påverkade inte några av de saker vi mätte. Det är troligt att det inte var tillräckligt med enbart två dagar med sänkt nivå av UCP-2 för att den kompensatoriska frikopplingen via ATP/ADP-transportören skulle ge mätbara effekter på njurens funktion.

Studie 1-5 etablerade att diabetes orsakar mitokondriell frikoppling via UCP-2 som då ökar syrgaskonsumtionen i njuren. Men i diabetesnefropati är det svårt att skilja effekterna av en sänkt syrgasnivå från effekterna av högt blodsocker och oxidativ stress. Kan den ökade syrgaskonsumtionen i mitokondrierna minska mängden syrgas i njuren så pass mycket att det bidrar till njurskador?

I studie 6 använde vi dinitrofenol (DNP), en kemisk mitokondriell frikopplare som ökar mitokondriens syrgaskonsumtion. DNP ändrar inte blodsockernivån hos djur och ökar inte heller den oxidativa stressen och effekten av en ökad syrgaskonsumtion kan därför studeras särskiljt från effekten av diabetes. Genom att administrera DNP till friska råttor under 30 dagar kunde vi sänka mängden syrgas i njuren och detta gav upphov till vävnadsskador och utsöndring av proteiner med urinen, tydliga och kliniskt kända tecken på njurskador. Studie visade alltså att ökad syrgaskonsumtion via mitokondriell frikoppling kan orsaka njurskador.

Slutsatser

UCP-2 är den enda formen av UCP-2 som finns i njuren och diabetes ökar nivån av UCP-2 i njuren vilket resulterar i mitokondriell frikoppling. Följden av detta är en ökad syrgaskonsumtion. Frikoppling via UCP-2 hos diabetiska djur är en så pass viktig mekanism att den kompenseras ifall den försvinner. Den ökade syrgaskonsumtion följer på mitokondriell frikoppling kan i sig leda till njurskador och denna avhandling drar därför slutsatsen att mitokondriell frikoppling är en bidragande mekanism i utvecklandet av njurskador till följd av diabetes.

Acknowledgements

This thesis was carried out at the Department of Medical Cell Biology, Division of Integrative Physiology, Uppsala University, Uppsala, Sweden. The work presented was supported by grants from the Swedish Research Council, the Swedish Diabetes Foundation, the Wallenberg Foundations, the Ernfors Foundation, the Rolf Luft Foundation for Diabetes Research, the Royal Society of Science and the Swedish Society for Medical Research.

Many people have helped with the production of this thesis, or with keeping me happy and sane. Wait, maybe that's the same thing? Anyhow, a lot of people should receive a big thank you for everything they have done!

My excellent supervisor **Fredrik Palm**. For always encouraging me and for your firm belief that everything is possible (and should be done immediately since it's so interesting). Without you as a supervisor I wouldn't be half as interested in science as I am! My co-supervisor, **Peter Hansell**. For always telling me the really annoying (but true!) statement "så är det ibland, det löser sig". Once you learn to listen to it, it actually works. That is, if you use it together with "Mahna Mahna"! Thanks also to my other co-supervisor, **Per Liss**, it is always fun when you do inspirational visits to the lab and discuss USB-2.

Angelica, for being the lab-Jedi that can find anything even if it's been lost since the eighties. For being there when the supervisors have gone mad and for feeding me with cookies! To **Ebba**, for being my own "Piglet" and for being a rock when I need it! And for laughing when I say weird things, making them funny when in truth they are only weird! **Liselott**, for "adjusting" my sense of the world and being great company! **Sara,** for excellent book discussions! **Stephanie**, for always lightening up the room and making me smile! **Lina**, I don't know anyone who does so many things at the same time but still manages to have time for a hug and some encouraging words!

To **Kerstin Brismar** and **Gustav Dallner** for a wonderful collaboration on study III and a great time in Brussels! The both of you (and Gustav's e-mails) always make me smile, thank you!

Thanks to **Christopher Wilcox** and **William Welch** (the Bill!) for the time I spent running around in your lab at Georgetown University, Washington DC, USA, doing experiments for study IV and V. For inspiring Monday meetings, journal clubs and Friday pizzas! I learned a lot and had a truly great time! Also, a big hug to **T-Bell**, **Carla**, **Glen**, **En-Yin**, **Shakil**, and **Dan** for company and help!

Big thank you to **Odra Noel** for letting me use her wonderful mitochondria art on the cover! I encourage everyone to visit www.odranoel.eu to see more mitochondria art.

To all my **co-authors** who have contributed to the different studies!

Thanks to my roommates over the years for good company and laughs! Especially my current roomies, **Ebba, Andreas** and **Micke Fluff** (The Beaver Brothers) and **Ehtesham**.

This job wouldn't be fun at all without all the people in the corridor sharing lunches, fika-times, weekends and making me smile. Thanks to **Evelina**, **Ulrika**, **Liza**, **Sara Massena**, **Gustaf**, **David**, **Andreas**, **Cecilia**, **Tomas**, **Xian** and **Annika**. Also, the "original" PhD-students who were there at the beginning, **Lina**, **Louise, Johan**, **Mattias**, **Andrei**, **Olof**, **Joel, Åsa, Sara,** and **Johanna**. Thanks to all PhD-students and seniors at the department for good discussions at Brain-pubs and Thursday seminars.

The seniors in the corridor: **Leif**, **Örjan**, **Erik**, **Ulf**, **Parri**, **Lena**, **P-O** and **Mia** – together you represent a pool of information with answers to everything a PhD-student can possibly think of. This includes (other than science questions of course): what books you absolutely must have read, whether or not you are truly dead after four minutes, how to best release frustration, the importance of the perfect tea-cup and whether you push a scheduled time forward or backwards!

Thanks to **Olerud**, **Super-Nils** and **Rickard Fred** for teaching me the tips and tricks of western blotting.

To **Galne-Gunno**, **Stålis**, **Agneta**, **Marianne**, **Camilla**, **Shumin**, **Lina T** and **Björn** for guidance in the world of economy, administration, mail, teaching, computers and laboratory equipment.

To my wonderful friends, **Johanna**, **Alfhild**, **Linda**, **Emma** and **Anna-Karin**, for always listening and understanding, lunches at BMC and very much needed "tjejkvällar".

Tack till underbara **mamma** och **pappa** som alltid finns där! Det är ett välbehövligt andningshål att komma hem till Hjälsta ibland och tänka på något annat än forskning! Till **Edvin** och **Linda** – de bästa nöffisarna i landet, **John** och **Helena** som håller Gotland flytande och **Liselott** och **Fredrik** som håller Göteborg glatt! Ni är alltid uppmuntrande och stöttande, tack för det!

Givetvis till **farmor** och **farfar**, ni är helt underbara och är mina idoler!

Till min extra familj, **Lena**, **Per-Ola** och **Karin**. Det är alltid underbart att gömma sig i stugan under en massa filtar och yrka på att vädret absolut (!) är för dåligt för att kunna åka skidor, ge med sig efter mycket tjat, traggla sig upp till Jaktstugan och sedan dratta på rumpan på vägen ner. Av någon underlig anledning så mår man väldigt bra av det! Till **Anita**, **Leif** och **Emy**, er blir man alltid glad av att träffa!

Patrik, du gör mig lycklig! Mer än så behöver väl knappast sägas.

Uppsala,
2012-02-06

"I'm glad I did it, partly because it was worth it, but mostly because I shall never have to do it again"
Mark Twain (1835-1910)

References

1. Thaysen, J.H., N.A. Lassen, and O. Munck, *Sodium transport and oxygen consumption in the mammalian kidney.* Nature, 1961. 190: p. 919-21.
2. Cohen, J. and D. Kamm, *Renal metabolism: Relation to renal function.* In: Brenner B, Rector F, Eds. The Kidney, 1985: p. 144-248.
3. Brezis, M., S.N. Heyman, and F.H. Epstein, *Determinants of intrarenal oxygenation. II. Hemodynamic effects.* Am J Physiol, 1994. 267(6 Pt 2): p. F1063-8.
4. Deng, A., et al., *Oxygen consumption in the kidney: effects of nitric oxide synthase isoforms and angiotensin II.* Kidney Int, 2005. 68(2): p. 723-30.
5. Aukland, K. and J. Krog, *Renal oxygen tension.* Nature, 1960. 188: p. 671.
6. Leichtweiss, H.P., et al., *The oxygen supply of the rat kidney: measurements of intrarenal pO2.* Pflugers Arch, 1969. 309(4): p. 328-49.
7. Levy, M.N. and G. Sauceda, *Diffusion of oxygen from arterial to venous segments of renal capillaires.* Am J Physiol, 1959. 196(6): p. 1336-9.
8. Levy, M.N. and E.S. Imperial, *Oxygen shunting in renal cortical and medullary capillaries.* Am J Physiol, 1961. 200: p. 159-62.
9. Grassmann, A., et al., *ESRD patients in 2004: global overview of patient numbers, treatment modalities and associated trends.* Nephrol Dial Transplant, 2005. 20(12): p. 2587-93.
10. Brand, M.D., et al., *The basal proton conductance of mitochondria depends on adenine nucleotide translocase content.* Biochem J, 2005. 392(Pt 2): p. 353-62.
11. Shabalina, I.G., et al., *Carboxyatractyloside effects on brown-fat mitochondria imply that the adenine nucleotide translocator isoforms ANT1 and ANT2 may be responsible for basal and fatty-acid-induced uncoupling respectively.* Biochem J, 2006. 399(3): p. 405-14.
12. Rolfe, D.F. and M.D. Brand, *Contribution of mitochondrial proton leak to skeletal muscle respiration and to standard metabolic rate.* Am J Physiol, 1996. 271(4 Pt 1): p. C1380-9.
13. Brand, M.D., et al., *The significance and mechanism of mitochondrial proton conductance.* Int J Obes Relat Metab Disord, 1999. 23 Suppl 6: p. S4-11.
14. Kroemer, G., N. Zamzami, and S.A. Susin, *Mitochondrial control of apoptosis.* Immunol Today, 1997. 18(1): p. 44-51.
15. Gunter, T.E., et al., *Mitochondrial calcium transport: mechanisms and functions.* Cell Calcium, 2000. 28(5-6): p. 285-96.
16. Jouaville, L.S., et al., *Synchronization of calcium waves by mitochondrial substrates in Xenopus laevis oocytes.* Nature, 1995. 377(6548): p. 438-41.
17. St-Pierre, J., et al., *Topology of superoxide production from different sites in the mitochondrial electron transport chain.* J Biol Chem, 2002. 277(47): p. 44784-90.
18. Kushnareva, Y., A.N. Murphy, and A. Andreyev, *Complex I-mediated reactive oxygen species generation: modulation by cytochrome c and NAD(P)+ oxidation-reduction state.* Biochem J, 2002. 368(Pt 2): p. 545-53.

19. Miwa, S., et al., *Superoxide and hydrogen peroxide production by Drosophila mitochondria.* Free Radic Biol Med, 2003. 35(8): p. 938-48.
20. Li, Y., et al., *Dilated cardiomyopathy and neonatal lethality in mutant mice lacking manganese superoxide dismutase.* Nat Genet, 1995. 11(4): p. 376-81.
21. Connor, K.M., et al., *Mitochondrial H2O2 regulates the angiogenic phenotype via PTEN oxidation.* J Biol Chem, 2005. 280(17): p. 16916-24.
22. Guzy, R.D., et al., *Mitochondrial complex III is required for hypoxia-induced ROS production and cellular oxygen sensing.* Cell Metab, 2005. 1(6): p. 401-8.
23. Sanjuan-Pla, A., et al., *A targeted antioxidant reveals the importance of mitochondrial reactive oxygen species in the hypoxic signaling of HIF-1alpha.* FEBS Lett, 2005. 579(12): p. 2669-74.
24. Bjelakovic, G., et al., *Antioxidant supplements for prevention of mortality in healthy participants and patients with various diseases.* Cochrane Database Syst Rev, 2008(2): p. CD007176.
25. Omenn, G.S., et al., *Effects of a combination of beta carotene and vitamin A on lung cancer and cardiovascular disease.* N Engl J Med, 1996. 334(18): p. 1150-5.
26. Ford, E.S., W.H. Giles, and W.H. Dietz, *Prevalence of the metabolic syndrome among US adults: findings from the third National Health and Nutrition Examination Survey.* Jama, 2002. 287(3): p. 356-9.
27. Wild, S., et al., *Global prevalence of diabetes: estimates for the year 2000 and projections for 2030.* Diabetes Care, 2004. 27(5): p. 1047-53.
28. Hasslacher, C., et al., *Similar risks of nephropathy in patients with type I or type II diabetes mellitus.* Nephrol Dial Transplant, 1989. 4(10): p. 859-63.
29. McCullough, P.A., et al., *Independent components of chronic kidney disease as a cardiovascular risk state: results from the Kidney Early Evaluation Program (KEEP).* Arch Intern Med, 2007. 167(11): p. 1122-9.
30. Foley, R.N. and A.J. Collins, *End-stage renal disease in the United States: an update from the United States Renal Data System.* J Am Soc Nephrol, 2007. 18(10): p. 2644-8.
31. Valmadrid, C.T., et al., *The risk of cardiovascular disease mortality associated with microalbuminuria and gross proteinuria in persons with older-onset diabetes mellitus.* Arch Intern Med, 2000. 160(8): p. 1093-100.
32. Mackensen-Haen, S., et al., *Correlations between renal cortical interstitial fibrosis, atrophy of the proximal tubules and impairment of the glomerular filtration rate.* Clin Nephrol, 1981. 15(4): p. 167-71.
33. Rudberg, S., B. Persson, and G. Dahlquist, *Increased glomerular filtration rate as a predictor of diabetic nephropathy--an 8-year prospective study.* Kidney Int, 1992. 41(4): p. 822-8.
34. O'Donnell, M.P., B.L. Kasiske, and W.F. Keane, *Glomerular hemodynamic and structural alterations in experimental diabetes mellitus.* Faseb J, 1988. 2(8): p. 2339-47.
35. Ruggenenti, P., et al., *Urinary protein excretion rate is the best independent predictor of ESRF in non-diabetic proteinuric chronic nephropathies. "Gruppo Italiano di Studi Epidemiologici in Nefrologia" (GISEN).* Kidney Int, 1998. 53(5): p. 1209-16.
36. Hunsicker, L.G., et al., *Predictors of the progression of renal disease in the Modification of Diet in Renal Disease Study.* Kidney Int, 1997. 51(6): p. 1908-19.
37. Mauer, S.M., M.W. Steffes, and D.M. Brown, *The kidney in diabetes.* Am J Med, 1981. 70(3): p. 603-12.

38. Brito, P.L., et al., *Proximal tubular basement membrane width in insulin-dependent diabetes mellitus.* Kidney Int, 1998. 53(3): p. 754-61.
39. Katz, A., et al., *An increase in the cell component of the cortical interstitium antedates interstitial fibrosis in type 1 diabetic patients.* Kidney Int, 2002. 61(6): p. 2058-66.
40. Steffes, M.W., et al., *Cell and matrix components of the glomerular mesangium in type I diabetes.* Diabetes, 1992. 41(6): p. 679-84.
41. Osterby, R., et al., *A strong correlation between glomerular filtration rate and filtration surface in diabetic nephropathy.* Diabetologia, 1988. 31(5): p. 265-70.
42. Mauer, M. and K. Drummond, *The early natural history of nephropathy in type 1 diabetes: I. Study design and baseline characteristics of the study participants.* Diabetes, 2002. 51(5): p. 1572-9.
43. *The effect of intensive treatment of diabetes on the development and progression of long-term complications in insulin-dependent diabetes mellitus. The Diabetes Control and Complications Trial Research Group.* N Engl J Med, 1993. 329(14): p. 977-86.
44. *Sustained effect of intensive treatment of type 1 diabetes mellitus on development and progression of diabetic nephropathy: the Epidemiology of Diabetes Interventions and Complications (EDIC) study.* Jama, 2003. 290(16): p. 2159-67.
45. Alaveras, A.E., et al., *Promoters of progression of diabetic nephropathy: the relative roles of blood glucose and blood pressure control.* Nephrol Dial Transplant, 1997. 12 Suppl 2: p. 71-4.
46. Vallon, V., *The proximal tubule in the pathophysiology of the diabetic kidney.* Am J Physiol Regul Integr Comp Physiol. 300(5): p. R1009-22.
47. Palm, F., et al., *Diabetes-induced decrease in renal oxygen tension: effects of an altered metabolism.* Adv Exp Med Biol, 2006. 578: p. 161-6.
48. Nishikawa, T., D. Edelstein, and M. Brownlee, *The missing link: a single unifying mechanism for diabetic complications.* Kidney Int Suppl, 2000. 77: p. S26-30.
49. Nishikawa, T., et al., *Normalizing mitochondrial superoxide production blocks three pathways of hyperglycaemic damage.* Nature, 2000. 404(6779): p. 787-90.
50. Forbes, J.M., M.T. Coughlan, and M.E. Cooper, *Oxidative stress as a major culprit in kidney disease in diabetes.* Diabetes, 2008. 57(6): p. 1446-54.
51. Baynes, J.W., *Role of oxidative stress in development of complications in diabetes.* Diabetes, 1991. 40(4): p. 405-12.
52. Peixoto, E.B., et al., *Antioxidant SOD mimetic prevents NADPH oxidase-induced oxidative stress and renal damage in the early stage of experimental diabetes and hypertension.* Am J Nephrol, 2009. 29(4): p. 309-18.
53. Palm, F., et al., *Reactive oxygen species cause diabetes-induced decrease in renal oxygen tension.* Diabetologia, 2003. 46(8): p. 1153-60.
54. Haidara, M.A., et al., *Evaluation of the effect of oxidative stress and vitamin E supplementation on renal function in rats with streptozotocin-induced Type 1 diabetes.* J Diabetes Complications, 2009. 23(2): p. 130-6.
55. Brownlee, M., *Biochemistry and molecular cell biology of diabetic complications.* Nature, 2001. 414(6865): p. 813-20.
56. Lee, S.M. and R. Bressler, *Prevention of diabetic nephropathy by diet control in the db/db mouse.* Diabetes, 1981. 30(2): p. 106-11.
57. Fujita, H., et al., *Reduction of renal superoxide dismutase in progressive diabetic nephropathy.* J Am Soc Nephrol, 2009. 20(6): p. 1303-13.

58. Ghosh, S., et al., *Moderate exercise attenuates caspase-3 activity, oxidative stress, and inhibits progression of diabetic renal disease in db/db mice.* Am J Physiol Renal Physiol, 2009. 296(4): p. F700-8.
59. Craven, P.A., et al., *Effects of supplementation with vitamin C or E on albuminuria, glomerular TGF-beta, and glomerular size in diabetes.* J Am Soc Nephrol, 1997. 8(9): p. 1405-14.
60. Koya, D., et al., *Effects of antioxidants in diabetes-induced oxidative stress in the glomeruli of diabetic rats.* J Am Soc Nephrol, 2003. 14(8 Suppl 3): p. S250-3.
61. Marra, G., et al., *Early increase of oxidative stress and reduced antioxidant defenses in patients with uncomplicated type 1 diabetes: a case for gender difference.* Diabetes Care, 2002. 25(2): p. 370-5.
62. Opara, E.C., et al., *Depletion of total antioxidant capacity in type 2 diabetes.* Metabolism, 1999. 48(11): p. 1414-7.
63. Alkhalaf, A., et al., *A double-blind, randomized, placebo-controlled clinical trial on benfotiamine treatment in patients with diabetic nephropathy.* Diabetes Care. 33(7): p. 1598-601.
64. Lonn, E., et al., *Effects of vitamin E on cardiovascular and microvascular outcomes in high-risk patients with diabetes: results of the HOPE study and MICRO-HOPE substudy.* Diabetes Care, 2002. 25(11): p. 1919-27.
65. Asaba, K., et al., *Effects of NADPH oxidase inhibitor in diabetic nephropathy.* Kidney Int, 2005. 67(5): p. 1890-8.
66. Tojo, A., K. Asaba, and M.L. Onozato, *Suppressing renal NADPH oxidase to treat diabetic nephropathy.* Expert Opin Ther Targets, 2007. 11(8): p. 1011-8.
67. Munusamy, S. and L.A. MacMillan-Crow, *Mitochondrial superoxide plays a crucial role in the development of mitochondrial dysfunction during high glucose exposure in rat renal proximal tubular cells.* Free Radic Biol Med, 2009. 46(8): p. 1149-57.
68. Starkov, A.A. and G. Fiskum, *Regulation of brain mitochondrial H2O2 production by membrane potential and NAD(P)H redox state.* J Neurochem, 2003. 86(5): p. 1101-7.
69. Quijano, C., et al., *Enhanced mitochondrial superoxide in hyperglycemic endothelial cells: direct measurements and formation of hydrogen peroxide and peroxynitrite.* Am J Physiol Heart Circ Physiol, 2007. 293(6): p. H3404-14.
70. Korshunov, S.S., V.P. Skulachev, and A.A. Starkov, *High protonic potential actuates a mechanism of production of reactive oxygen species in mitochondria.* FEBS Lett, 1997. 416(1): p. 15-8.
71. Lambert, A.J. and M.D. Brand, *Superoxide production by NADH:ubiquinone oxidoreductase (complex I) depends on the pH gradient across the mitochondrial inner membrane.* Biochem J, 2004. 382(Pt 2): p. 511-7.
72. Harman, D., *Aging: a theory based on free radical and radiation chemistry.* J Gerontol, 1956. 11(3): p. 298-300.
73. Skulachev, V.P., *Uncoupling: new approaches to an old problem of bioenergetics.* Biochim Biophys Acta, 1998. 1363(2): p. 100-24.
74. Friederich, M., P. Hansell, and F. Palm, *Diabetes, oxidative stress, nitric oxide and mitochondria function.* Curr Diabetes Rev, 2009. 5(2): p. 120-44.
75. Miwa, S. and M.D. Brand, *Mitochondrial matrix reactive oxygen species production is very sensitive to mild uncoupling.* Biochem Soc Trans, 2003. 31(Pt 6): p. 1300-1.

76. Duval, C., et al., *Increased reactive oxygen species production with antisense oligonucleotides directed against uncoupling protein 2 in murine endothelial cells.* Biochem Cell Biol, 2002. 80(6): p. 757-64.
77. Nicholls, D.G., *Hamster brown-adipose-tissue mitochondria. Purine nucleotide control of the ion conductance of the inner membrane, the nature of the nucleotide binding site.* Eur J Biochem, 1976. 62(2): p. 223-8.
78. Nicholls, D.G. and R.M. Locke, *Thermogenic mechanisms in brown fat.* Physiol Rev, 1984. 64(1): p. 1-64.
79. Giardina, T.M., et al., *Uncoupling protein-2 accumulates rapidly in the inner mitochondrial membrane during mitochondrial reactive oxygen stress in macrophages.* Biochim Biophys Acta, 2008. 1777(2): p. 118-29.
80. Fleury, C., et al., *Uncoupling protein-2: a novel gene linked to obesity and hyperinsulinemia.* Nat Genet, 1997. 15(3): p. 269-72.
81. Alan, L., et al., *Absolute levels of transcripts for mitochondrial uncoupling proteins UCP2, UCP3, UCP4, and UCP5 show different patterns in rat and mice tissues.* J Bioenerg Biomembr, 2009. 41(1): p. 71-8.
82. Jezek, P., et al., *Existence of uncoupling protein-2 antigen in isolated mitochondria from various tissues.* FEBS Lett, 1999. 455(1-2): p. 79-82.
83. Vidal-Puig, A., et al., *UCP3: an uncoupling protein homologue expressed preferentially and abundantly in skeletal muscle and brown adipose tissue.* Biochem Biophys Res Commun, 1997. 235(1): p. 79-82.
84. Sanchis, D., et al., *BMCP1, a novel mitochondrial carrier with high expression in the central nervous system of humans and rodents, and respiration uncoupling activity in recombinant yeast.* J Biol Chem, 1998. 273(51): p. 34611-5.
85. Yu, X.X., et al., *Characterization of novel UCP5/BMCP1 isoforms and differential regulation of UCP4 and UCP5 expression through dietary or temperature manipulation.* Faseb J, 2000. 14(11): p. 1611-8.
86. Jaburek, M., et al., *Transport function and regulation of mitochondrial uncoupling proteins 2 and 3.* J Biol Chem, 1999. 274(37): p. 26003-7.
87. Negre-Salvayre, A., et al., *A role for uncoupling protein-2 as a regulator of mitochondrial hydrogen peroxide generation.* Faseb J, 1997. 11(10): p. 809-15.
88. Echtay, K.S., et al., *Uncoupling proteins 2 and 3 are highly active H(+) transporters and highly nucleotide sensitive when activated by coenzyme Q (ubiquinone).* Proc Natl Acad Sci U S A, 2001. 98(4): p. 1416-21.
89. Echtay, K.S., et al., *Superoxide activates mitochondrial uncoupling proteins.* Nature, 2002. 415(6867): p. 96-9.
90. Klingenberg, M., et al., *Structure-function relationship in UCP1.* Int J Obes Relat Metab Disord, 1999. 23 Suppl 6: p. S24-9.
91. Skulachev, V.P., *Fatty acid circuit as a physiological mechanism of uncoupling of oxidative phosphorylation.* FEBS Lett, 1991. 294(3): p. 158-62.
92. Klingenberg, M. and S.G. Huang, *Structure and function of the uncoupling protein from brown adipose tissue.* Biochim Biophys Acta, 1999. 1415(2): p. 271-96.
93. Garlid, K.D., M. Jaburek, and P. Jezek, *Mechanism of uncoupling protein action.* Biochem Soc Trans, 2001. 29(Pt 6): p. 803-6.
94. Garlid, K.D., et al., *On the mechanism of fatty acid-induced proton transport by mitochondrial uncoupling protein.* J Biol Chem, 1996. 271(5): p. 2615-20.
95. Jezek, P., *Fatty acid interaction with mitochondrial uncoupling proteins.* J Bioenerg Biomembr, 1999. 31(5): p. 457-66.
96. Breen, E.P., et al., *On the mechanism of mitochondrial uncoupling protein 1 function.* J Biol Chem, 2006. 281(4): p. 2114-9.

97. Arsenijevic, D., et al., *Disruption of the uncoupling protein-2 gene in mice reveals a role in immunity and reactive oxygen species production.* Nat Genet, 2000. 26(4): p. 435-9.
98. Vidal-Puig, A.J., et al., *Energy metabolism in uncoupling protein 3 gene knockout mice.* J Biol Chem, 2000. 275(21): p. 16258-66.
99. Gimeno, R.E., et al., *Cloning and characterization of an uncoupling protein homolog: a potential molecular mediator of human thermogenesis.* Diabetes, 1997. 46(5): p. 900-6.
100. Basu Ball, W., et al., *Uncoupling protein 2 negatively regulates mitochondrial reactive oxygen species generation and induces phosphatase-mediated anti-inflammatory response in experimental visceral leishmaniasis.* J Immunol. 187(3): p. 1322-32.
101. Rousset, S., et al., *The uncoupling protein 2 modulates the cytokine balance in innate immunity.* Cytokine, 2006. 35(3-4): p. 135-42.
102. Vincent, A.M., et al., *Uncoupling proteins prevent glucose-induced neuronal oxidative stress and programmed cell death.* Diabetes, 2004. 53(3): p. 726-34.
103. Mattiasson, G., et al., *Uncoupling protein-2 prevents neuronal death and diminishes brain dysfunction after stroke and brain trauma.* Nat Med, 2003. 9(8): p. 1062-8.
104. Echtay, K.S., et al., *A signalling role for 4-hydroxy-2-nonenal in regulation of mitochondrial uncoupling.* Embo J, 2003. 22(16): p. 4103-10.
105. Echtay, K.S., et al., *Superoxide activates mitochondrial uncoupling protein 2 from the matrix side. Studies using targeted antioxidants.* J Biol Chem, 2002. 277(49): p. 47129-35.
106. Rousset, S., et al., *UCP2 is a mitochondrial transporter with an unusual very short half-life.* FEBS Lett, 2007. 581(3): p. 479-82.
107. Krauss, S., et al., *Superoxide-mediated activation of uncoupling protein 2 causes pancreatic beta cell dysfunction.* J Clin Invest, 2003. 112(12): p. 1831-42.
108. Korner, A., et al., *Increased renal metabolism in diabetes. Mechanism and functional implications.* Diabetes, 1994. 43(5): p. 629-33.
109. Edlund, J., et al., *Reduced oxygenation in diabetic rat kidneys measured by T2* weighted magnetic resonance micro-imaging.* Adv Exp Med Biol, 2009. 645: p. 199-204.
110. Rosenberger, C., et al., *Adaptation to hypoxia in the diabetic rat kidney.* Kidney Int, 2008. 73(1): p. 34-42.
111. dos Santos, E.A., et al., *Early changes with diabetes in renal medullary hemodynamics as evaluated by fiberoptic probes and BOLD magnetic resonance imaging.* Invest Radiol, 2007. 42(3): p. 157-62.
112. Ries, M., et al., *Renal diffusion and BOLD MRI in experimental diabetic nephropathy. Blood oxygen level-dependent.* J Magn Reson Imaging, 2003. 17(1): p. 104-13.
113. Inoue, T., et al., *Noninvasive evaluation of kidney hypoxia and fibrosis using magnetic resonance imaging.* J Am Soc Nephrol. 22(8): p. 1429-34.
114. Fine, L.G., C. Orphanides, and J.T. Norman, *Progressive renal disease: the chronic hypoxia hypothesis.* Kidney Int Suppl, 1998. 65: p. S74-8.
115. Ohtomo, S., et al., *Cobalt ameliorates renal injury in an obese, hypertensive type 2 diabetes rat model.* Nephrol Dial Transplant, 2008. 23(4): p. 1166-72.
116. Nangaku, M., *Chronic hypoxia and tubulointerstitial injury: a final common pathway to end-stage renal failure.* J Am Soc Nephrol, 2006. 17(1): p. 17-25.
117. Nangaku, M., *Hypoxia and tubulointerstitial injury: a final common pathway to end-stage renal failure.* Nephron Exp Nephrol, 2004. 98(1): p. e8-12.

118. Mimura, I. and M. Nangaku, *The suffocating kidney: tubulointerstitial hypoxia in end-stage renal disease.* Nat Rev Nephrol. 6(11): p. 667-78.
119. Singh, D.K., P. Winocour, and K. Farrington, *Mechanisms of disease: the hypoxic tubular hypothesis of diabetic nephropathy.* Nat Clin Pract Nephrol, 2008. 4(4): p. 216-26.
120. Palm, F. and L. Nordquist, *Renal tubulointerstitial hypoxia: cause and consequence of kidney dysfunction.* Clin Exp Pharmacol Physiol. 38(7): p. 424-30.
121. Schnedl, W.J., et al., *STZ transport and cytotoxicity. Specific enhancement in GLUT2-expressing cells.* Diabetes, 1994. 43(11): p. 1326-33.
122. Uchigata, Y., et al., *Protection by superoxide dismutase, catalase, and poly(ADP-ribose) synthetase inhibitors against alloxan- and streptozotocin-induced islet DNA strand breaks and against the inhibition of proinsulin synthesis.* J Biol Chem, 1982. 257(11): p. 6084-8.
123. Gandy, S.E., M.G. Buse, and R.K. Crouch, *Protective role of superoxide dismutase against diabetogenic drugs.* J Clin Invest, 1982. 70(3): p. 650-8.
124. Palm, F., et al., *Differentiating between effects of streptozotocin per se and subsequent hyperglycemia on renal function and metabolism in the streptozotocin-diabetic rat model.* Diabetes Metab Res Rev, 2004. 20(6): p. 452-9.
125. Palm, F., et al., *Transient glomerular hyperfiltration in the streptozotocin-diabetic Wistar Furth rat.* Ups J Med Sci, 2001. 106(3): p. 175-82.
126. Yang, Y., et al., *Rapamycin prevents early steps of the development of diabetic nephropathy in rats.* Am J Nephrol, 2007. 27(5): p. 495-502.
127. Masaki, T., et al., *Impaired response of UCP family to cold exposure in diabetic (db/db) mice.* Am J Physiol Regul Integr Comp Physiol, 2000. 279(4): p. R1305-9.
128. Kobayashi, K., et al., *The db/db mouse, a model for diabetic dyslipidemia: molecular characterization and effects of Western diet feeding.* Metabolism, 2000. 49(1): p. 22-31.
129. Coleman, D.L. and K.P. Hummel, *Hyperinsulinemia in pre-weaning diabetes (db) mice.* Diabetologia, 1974. 10 Suppl: p. 607-10.
130. Gartner, K., *Glomerular hyperfiltration during the onset of diabetes mellitus in two strains of diabetic mice (c57bl/6j db/db and c57bl/ksj db/db).* Diabetologia, 1978. 15(1): p. 59-63.
131. Hong, S.W., et al., *Increased glomerular and tubular expression of transforming growth factor-beta1, its type II receptor, and activation of the Smad signaling pathway in the db/db mouse.* Am J Pathol, 2001. 158(5): p. 1653-63.
132. Cohen, M.P., G.T. Lautenslager, and C.W. Shearman, *Increased urinary type IV collagen marks the development of glomerular pathology in diabetic d/db mice.* Metabolism, 2001. 50(12): p. 1435-40.
133. Cohen, M.P., et al., *Evolution of renal function abnormalities in the db/db mouse that parallels the development of human diabetic nephropathy.* Exp Nephrol, 1996. 4(3): p. 166-71.
134. Stridh, S., et al., *C-peptide normalizes glomerular filtration rate in hyperfiltrating conscious diabetic rats.* Adv Exp Med Biol, 2009. 645: p. 219-25.
135. Gabrielsson, J. and P. Weiner, *Non-compartmental Analysis, in: Pharmakokinetic and Pharmakodynamic Data Analysis: Concenpts and Applications.* Swedish Pharmaceutical Press, Stockholm, 2006.
136. Scaduto, R.C., Jr. and L.W. Grotyohann, *Measurement of mitochondrial membrane potential using fluorescent rhodamine derivatives.* Biophys J, 1999. 76(1 Pt 1): p. 469-77.

137. Mootha, V.K., A.E. Arai, and R.S. Balaban, *Maximum oxidative phosphorylation capacity of the mammalian heart.* Am J Physiol, 1997. 272(2 Pt 2): p. H769-75.
138. Tanaka, T., et al., *Induction of protective genes by cobalt ameliorates tubulointerstitial injury in the progressive Thy1 nephritis.* Kidney Int, 2005. 68(6): p. 2714-25.
139. Modriansky, M., et al., *Identification by site-directed mutagenesis of three arginines in uncoupling protein that are essential for nucleotide binding and inhibition.* J Biol Chem, 1997. 272(40): p. 24759-62.
140. Paulik, M.A., et al., *Development of infrared imaging to measure thermogenesis in cell culture: thermogenic effects of uncoupling protein-2, troglitazone, and beta-adrenoceptor agonists.* Pharm Res, 1998. 15(6): p. 944-9.
141. Himms-Hagen, J. and M.E. Harper, *Biochemical aspects of the uncoupling proteins: view from the chair.* Int J Obes Relat Metab Disord, 1999. 23 Suppl 6: p. S30-2.
142. Kelley, D.E., et al., *Dysfunction of mitochondria in human skeletal muscle in type 2 diabetes.* Diabetes, 2002. 51(10): p. 2944-50.
143. Boudina, S., et al., *Reduced mitochondrial oxidative capacity and increased mitochondrial uncoupling impair myocardial energetics in obesity.* Circulation, 2005. 112(17): p. 2686-95.
144. Ritov, V.B., et al., *Deficiency of subsarcolemmal mitochondria in obesity and type 2 diabetes.* Diabetes, 2005. 54(1): p. 8-14.
145. Santos, D.L., et al., *Diabetes and mitochondrial oxidative stress: a study using heart mitochondria from the diabetic Goto-Kakizaki rat.* Mol Cell Biochem, 2003. 246(1-2): p. 163-70.
146. Couplan, E., et al., *No evidence for a basal, retinoic, or superoxide-induced uncoupling activity of the uncoupling protein 2 present in spleen or lung mitochondria.* J Biol Chem, 2002. 277(29): p. 26268-75.
147. Frei, B., M.C. Kim, and B.N. Ames, *Ubiquinol-10 is an effective lipid-soluble antioxidant at physiological concentrations.* Proc Natl Acad Sci U S A, 1990. 87(12): p. 4879-83.
148. Crane, F.L., et al., *Isolation of a quinone from beef heart mitochondria.* Biochim Biophys Acta, 1957. 25(1): p. 220-1.
149. Diomedi-Camassei, F., et al., *COQ2 nephropathy: a newly described inherited mitochondriopathy with primary renal involvement.* J Am Soc Nephrol, 2007. 18(10): p. 2773-80.
150. Yu, T., J.L. Robotham, and Y. Yoon, *Increased production of reactive oxygen species in hyperglycemic conditions requires dynamic change of mitochondrial morphology.* Proc Natl Acad Sci U S A, 2006. 103(8): p. 2653-8.
151. Mogensen, C.E., *Microalbuminuria predicts clinical proteinuria and early mortality in maturity-onset diabetes.* N Engl J Med, 1984. 310(6): p. 356-60.
152. Koulintchenko, M., Y. Konstantinov, and A. Dietrich, *Plant mitochondria actively import DNA via the permeability transition pore complex.* Embo J, 2003. 22(6): p. 1245-54.
153. Bevilacqua, L., et al., *Absence of uncoupling protein-3 leads to greater activation of an adenine nucleotide translocase-mediated proton conductance in skeletal muscle mitochondria from calorie restricted mice.* Biochim Biophys Acta. 1797(8): p. 1389-97.
154. Parascandola, J., *Dinitrophenol and bioenergetics: an historical perspective.* Mol Cell Biochem, 1974. 5(1-2): p. 69-77.
155. Horner, W.D., *A Study of Dinitrophenol and Its Relation to Cataract Formation.* Trans Am Ophthalmol Soc, 1941. 39: p. 405-37.

156. Caldeira da Silva, C.C., et al., *Mild mitochondrial uncoupling in mice affects energy metabolism, redox balance and longevity.* Aging Cell, 2008. 7(4): p. 552-60.
157. Muramatsu, M., et al., *Estimation of damaged tubular epithelium in renal allografts by determination of vimentin expression.* Int J Urol, 2004. 11(11): p. 954-62.
158. Grone, H.J., et al., *Coexpression of keratin and vimentin in damaged and regenerating tubular epithelia of the kidney.* Am J Pathol, 1987. 129(1): p. 1-8.
159. Tainter, M., W. Cutting, and D. Wood, *Dinitrophenol. Studies of blood, urine and tissues on dogs on continued medication and after acute fatal poisoning.* A.M.A Arch Pathol, 1934. 18: p. 881.
160. Beinhauer, L., *Urticaria following the use of dinitrophenol.* W V Med J, 1934. October: p. 466-477.
161. Imerman, S. and C. Imerman, *Dinitrophenol poisoning with thrombocytopenia, granulopenia, anemia and purpura complicated by lung abscess.* JAMA, 1936. 106: p. 1085-1088.
162. Wang, Y., et al., *Induction of monocyte chemoattractant protein-1 by albumin is mediated by nuclear factor kappaB in proximal tubule cells.* J Am Soc Nephrol, 1999. 10(6): p. 1204-13.
163. Tang, S., et al., *Albumin stimulates interleukin-8 expression in proximal tubular epithelial cells in vitro and in vivo.* J Clin Invest, 2003. 111(4): p. 515-27.
164. Haase, V.H., *Hypoxia-inducible factors in the kidney.* Am J Physiol Renal Physiol, 2006. 291(2): p. F271-81.
165. Maxwell, P., *HIF-1: an oxygen response system with special relevance to the kidney.* J Am Soc Nephrol, 2003. 14(11): p. 2712-22.
166. Harvey, A.J., K.L. Kind, and J.G. Thompson, *Effect of the oxidative phosphorylation uncoupler 2,4-dinitrophenol on hypoxia-inducible factor-regulated gene expression in bovine blastocysts.* Reprod Fertil Dev, 2004. 16(7): p. 665-73.
167. Weidemann, A. and R.S. Johnson, *Nonrenal regulation of EPO synthesis.* Kidney Int, 2009. 75(7): p. 682-8.
168. Evans, R.G., et al., *Stability of tissue PO2 in the face of altered perfusion: a phenomenon specific to the renal cortex and independent of resting renal oxygen consumption.* Clin Exp Pharmacol Physiol. 38(4): p. 247-54.
169. Johannesen, J., M. Lie, and F. Kiil, *Renal energy metabolism and sodium reabsorption after 2,4-dinitrophenol administration.* Am J Physiol, 1977. 233(3): p. F207-12.
170. Hochman, M.E., et al., *The prevalence and incidence of end-stage renal disease in Native American adults on the Navajo reservation.* Kidney Int, 2007. 71(9): p. 931-7.
171. Sayarlioglu, H., et al., *Nephropathy and retinopathy in type 2 diabetic patients living at moderately high altitude and sea level.* Ren Fail, 2005. 27(1): p. 67-71.

Acta Universitatis Upsaliensis

Digital Comprehensive Summaries of Uppsala Dissertations from the Faculty of Medicine 738

Editor: The Dean of the Faculty of Medicine

A doctoral dissertation from the Faculty of Medicine, Uppsala University, is usually a summary of a number of papers. A few copies of the complete dissertation are kept at major Swedish research libraries, while the summary alone is distributed internationally through the series Digital Comprehensive Summaries of Uppsala Dissertations from the Faculty of Medicine.

Distribution: publications.uu.se
urn:nbn:se:uu:diva-167815

ACTA
UNIVERSITATIS
UPSALIENSIS
UPPSALA
2012